

# Research in Flapping-wing flight of insect-like flyers

**Presented by: K.S. Yeo**

Department of Mechanical Engineering, National University of Singapore

2013 Fall Progress in Mathematical and Computational  
Studies on Science and Engineering Problems

November 11-13, 2013

308, Mathematics Research Centre, National Taiwan  
University



# Hovering Flight

## Insects – basic facts

- ❑ Insects are the most abundant of all terrestrial animals today.
- ❑ Insects were capable of powered flight more than  $300 \times 10^6$  years ago in the Upper Carboniferous period -  $100 \times 10^6$  years before the pterosaurs took to the air.
- ❑ The early insects (hexapods – 6-legged arthropods) of the geologic era were much larger than their counterparts today: dragonflies with wing spans  $> 0.7\text{m}$ . Many insects had wingspans ranging 0.2 to 0.5m.
- ❑  $> 99.9\%$  of insect species today are wing insects (pterygotes). There are  $> 10^6$  species of described wing insects of an estimated  $10^7$  species of insects.
- ❑ Insects of today are mostly  $< 10\text{ cm}$  in size and weigh  $< 2\text{-}3\text{ gm}$ . The smallest insects measure about 1 mm and have weight in the order of micrograms.

# Flight modes

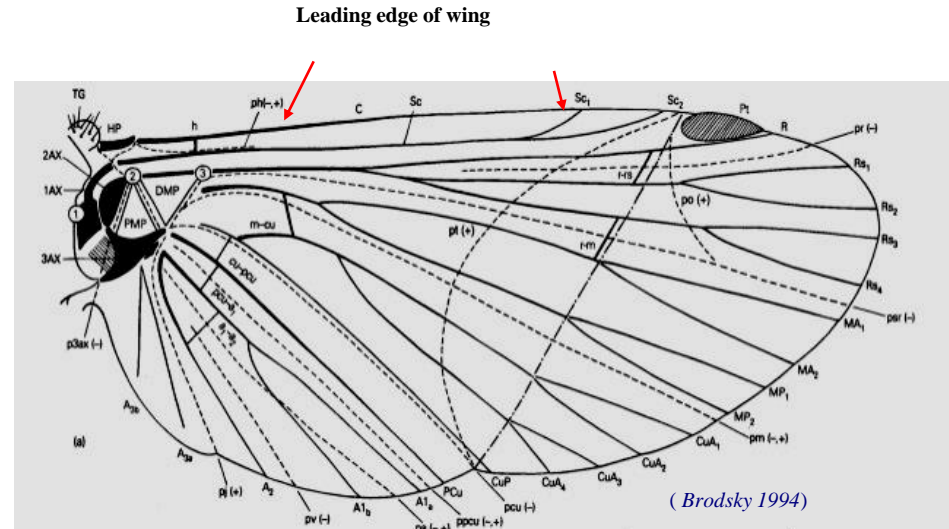
Terrestrial flyers	Primary Modes of flight
Airplanes	Gliding
Birds	Gliding; limited wing flapping*
Insects	Wing flapping; limited gliding**

\*Except hummingbirds; \*\*Except large insects.

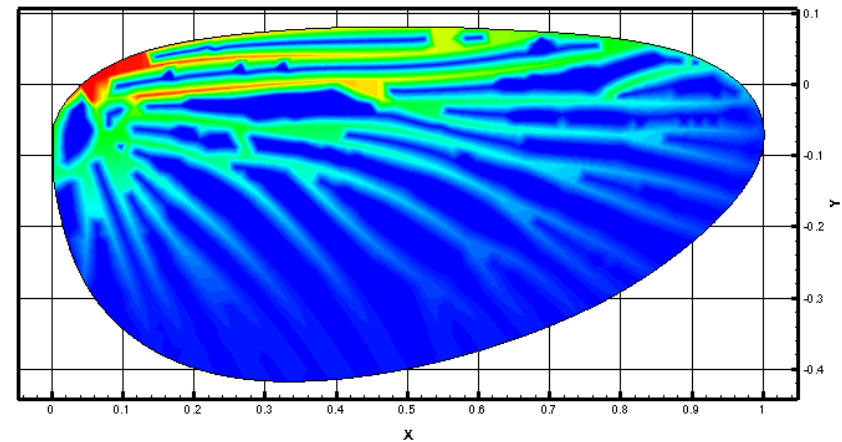
- Insects are the most accomplished among terrestrial flyers; many are able to hover for long periods, fly backwards, upside down, or even mate in mid-flight.
- The smaller an insect, the higher is the flapping frequency  
Wing beat frequency :10-1000 Hz  
Linear Speed up to 7 m/s (may be higher);  $Re \sim < 1$  to  $10^4$  (Birds:  $10^4$ - $10^7$ )

# Wings and wing action

- The typical insect wing
  - is a complex thin venated structures, with stiff front margin – the surface is not smooth, with vein protrusions, tiny spikes and hairs.
  - The wings usually constitute just a few % of total insect mass.

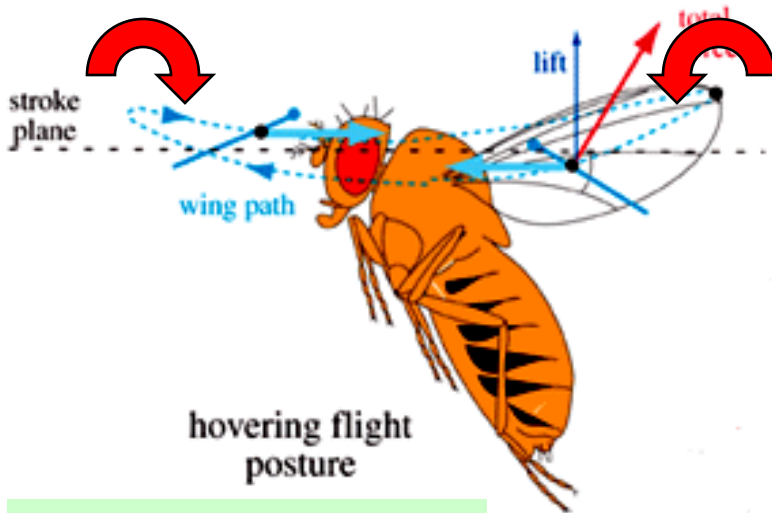


- Insects may have 2 wings or 4 wings.
- For many insects, the hind-wing may be coupled to the fore-wing and use as one during flight.



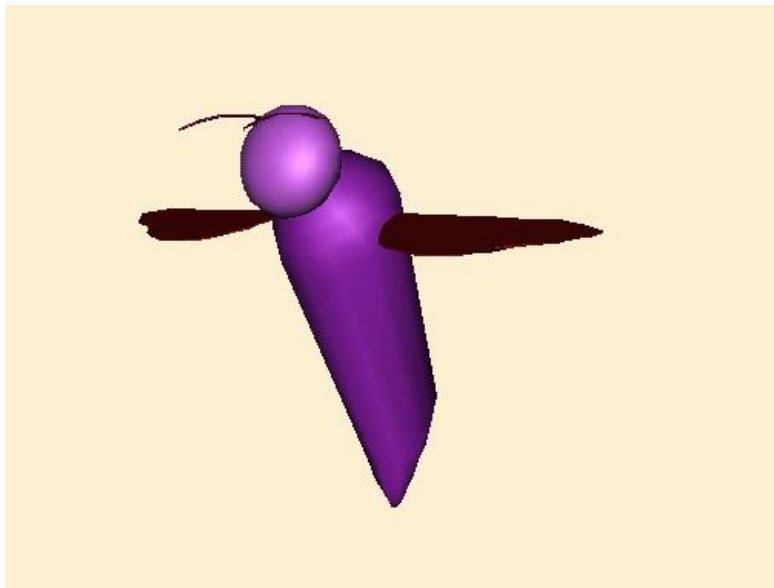
A computer model

# Wing action – single wing pair

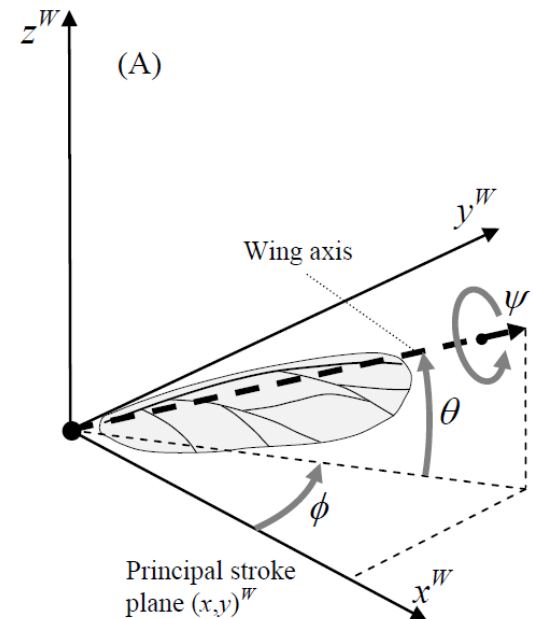


(From Dickinson, Berkeley)

- The flapping action of a wing comprises three actions:
  - Reciprocating sweeping /stroking action  $\angle \phi$  – downstroke and upstroke.
  - Elevation from principal/mean stroke/sweep plane  $\angle \theta$ .
  - Twisting of the wings  $\angle \psi$  (wing root rotation/flexibility).



Schematics of wing actions



# Unsteady Aerodynamics of flapping wings

- Research in the 1980s and 90s indicated that the conventional quasi-steady aerodynamic theory cannot adequately account for the ability of insects to fly, especially the smaller insects at very low linear speeds.
- *Unsteady* aerodynamic mechanisms that have been suggested or identified to date that could enhance lift generation include:
  - Leading edge vortex (LEV) – produced by large AoA and sharp leading edge)
  - Rotational lift (Enhanced circulation due to wing rotation near end of the strokes)
  - Wake capture
  - Acceleration effect
  - Clap-Fling mechanism (first identified for some very small insects *Encarsia Formosa* (Weis-Fogh 1973) but may also be applicable to some larger insects ( Clap-Peel of butterflies).
- In general, it is not possible to separate the contributions of all these possibly contributing effects to lift.
- These overall effect is very sensitive to kinematic details of wing motion.

# Flapping-wing research at ME Department, NUS

- ❑ Our work here comprises experimental modelling and computational modelling. It took us some time, amidst usual constraint of resources, to establish the measurement facilities and develop the computational tools
  
- ❑ Experimental Research: focus on force and flow measurements  
Facilities:
  - [2D flapping-wing rigs for force and DPIV measurements](#) →
  - [3D flapping-wing rig for force measurements \(large scale models\)](#) →
  - 3D flapping-wing rig for force and 3D PIV measurements (smaller scale models)-currently under development.
  
- ❑ Computational research: focus on
  - Development of suitable computational modelling tools.
  - Simulation flapping-wing aerodynamics and flight.



# Computational modelling of flapping aerodynamics

- ❑ The present talk will focus on recent computational work carried out at the ME Department, NUS.
- ❑ There are several groups that are very active on the computation front for many years:
  - Liu Hao (Chiba, Japan)
  - Sun Mao (BUAA, Beijing, China)
  - Wang J. (Cornell, USA)
  - Others
- ❑ Their works have primarily been concerned with flapping wings with fixed/prescribed kinematics (frequently derived from published experimental sources) and the lift that is generated.
- ❑ Focus of the present talk is on **free flight simulation**, which has not been much attempted.

# Free flight Simulation

- Why study free flight?
  - Lift is only the most basic requirement for flight, and of itself cannot explain why sustained flight is possible.
  - *Flight is quintessentially a dynamic condition* – more so when large unsteady forces and moments are generated by the flapping wings of a free body.
  - Sustained flight is possible only if the system of aerodynamic forces and moments acting on the flyers as a free body can be made dynamically stable in some sense.
  - Significantly, free flight study will better reflect the true conditions and requirements of flight and brings to the fore essential elements of both aerodynamics and its control.
  - Some free flight conditions are difficult to reproduce in laboratory, as the subject may not cooperate.
  
- In this presentation, we are concerned primarily with **free flight of flapping-wing insect-type flyers**. In particular I shall talk about some of the recent work that we have done on:
  - Free hovering flight
  - Forward/backward flight

# Brief outline of computational methodology

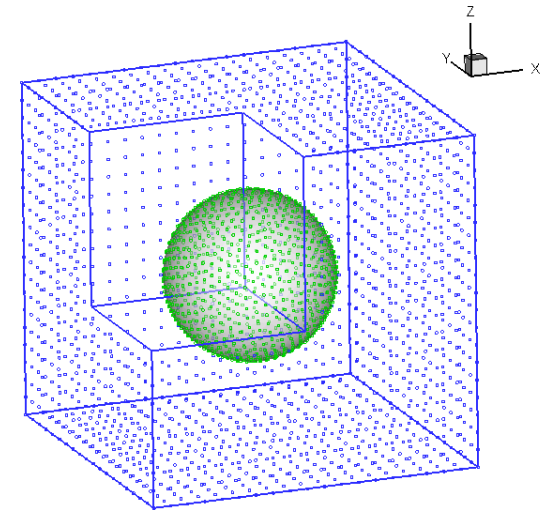
- The dynamics of the fluid is governed by the incompressible Navier-Stokes equations with arbitrary Lagrangian-Eulerian (ALE) convection.

$$\partial_t \mathbf{u} + (\mathbf{u} - \mathbf{u}_c) \cdot \nabla \mathbf{u} = -\nabla p + \frac{1}{\text{Re}} \nabla^2 \mathbf{u}$$

$$\nabla \cdot \mathbf{u} = 0$$

where  $\mathbf{u}_c$  is the velocity of node convection.

- The flow equations are discretized by conventional Finite difference and SVD-based Generalized Finite Difference (GFD) on a hybrid Cartesian-meshfree grid system; whereby *embedded bodies* are
  - Discretized by meshfree nodes and
  - Enclosed by a cloud of meshfree nodes.
- *Meshfree* here refers to the absence of nodal connectivity.



**Hybrid Cartesian  
cum meshfree grid**

# Fluid-body interaction

- Fluid body interaction leading to motion is governed by Newton's Laws:

$$\frac{d\mathbf{X}_C(t)}{dt} = \mathbf{V}_C(t)$$

$$\frac{d\mathbf{\Theta}(t)}{dt} = [\mathbf{K}(t)] \cdot \boldsymbol{\omega}(t)$$

$$\frac{d(M \cdot \mathbf{V}_C)}{dt} = -Mg \mathbf{i}_z + \int_{\Gamma(t)} [\boldsymbol{\sigma}] \cdot \mathbf{n} d\Gamma$$

$$\frac{d([\mathbf{I}(t)] \cdot \boldsymbol{\omega}(t))}{dt} = \int_{\Gamma(t)} (\mathbf{x} - \mathbf{X}_C(t)) \times ([\boldsymbol{\sigma}] \cdot \mathbf{n}) d\Gamma$$

$(\mathbf{X}_C, \mathbf{\Theta})$  : Position of centre of mass and Frame Orientation vector of Flyer

$(\mathbf{V}_C, \boldsymbol{\omega})$  : Linear and Angular Velocity vector of centre of mass

$(M \cdot \mathbf{V}_C)$  : Total Linear Momentum of composite body

$(\mathbf{I} \cdot \boldsymbol{\omega})$  : Total Angular Momentum of composite body

$[\boldsymbol{\sigma}]$  : Surface stress tensor

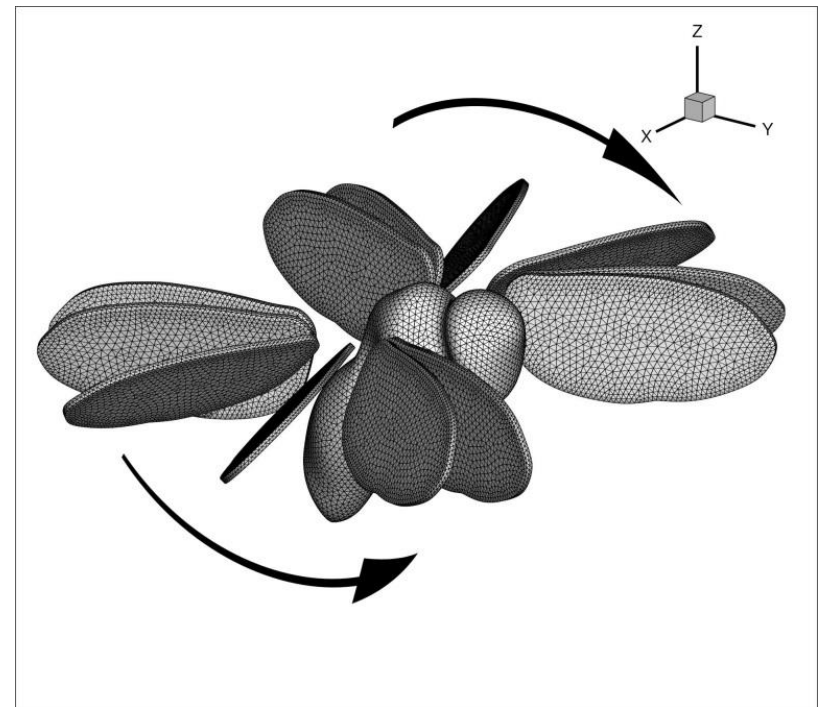
Velocity of body nodes in the current flyer configuration  $\Gamma(t, \mathbf{X}_C(t), \mathbf{\Theta}(t))$ .

$$\mathbf{u}(\mathbf{x}, t) = \mathbf{V}_C(t) + \boldsymbol{\omega}(t) \times (\mathbf{x} - \mathbf{X}_C(t)) + \mathbf{V}_{x/C}(t) \quad (\mathbf{x} \in \Gamma(t, \mathbf{X}_C(t), \mathbf{\Theta}(t)))$$

## (Contd.)

- Time integration of the fluid and body dynamics is carried out by the trapezoidal rule with
  - Projection method for fluid continuity,
  - Fixed-point iteration scheme for time-dependent to determine the time-dependent configuration of the flyer  $\Gamma(t, \mathbf{X}_c(t), \Theta(t))$ .

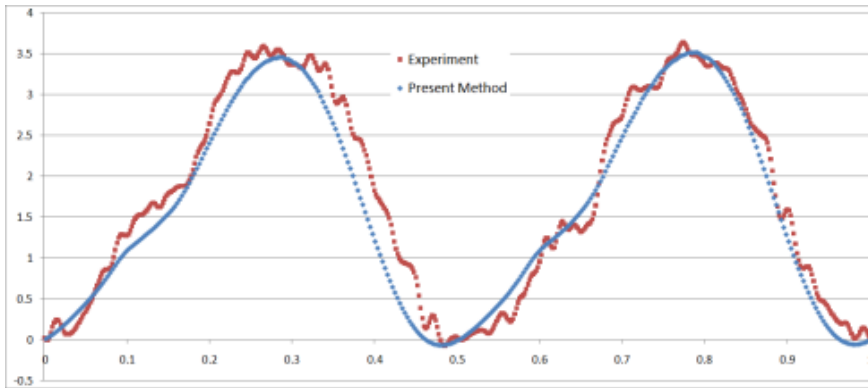
- The model flyer is assumed to be rigid except for specified/controlled motion of the wings within its body frame of flyer.



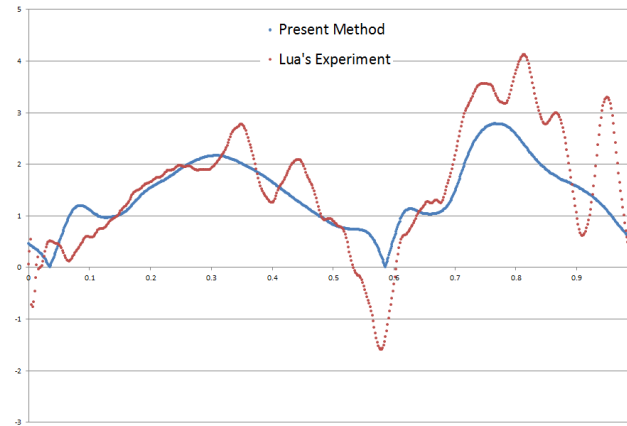
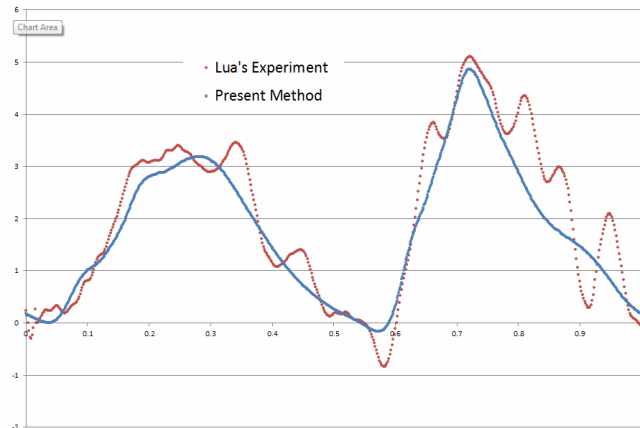
Discretization of a model flyer

# Validation study

- ❑ Codes tested on FSI problems
- ❑ Comparison with experiments



Lift for smooth sinusoidal wing action at  $Re = 150$ .



Lift and Drag forces for Fruit-fly wing action at  $Re = 200$ .

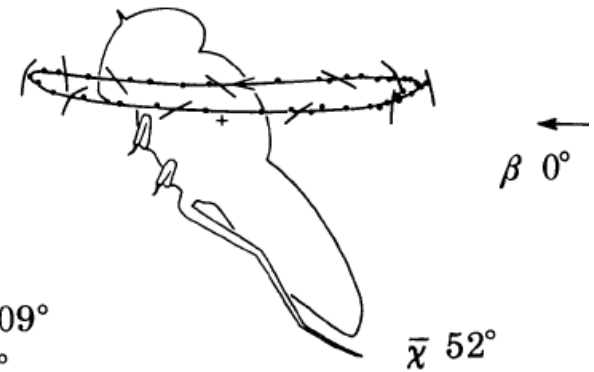
# Hovering flight

□ Hovering refers to a state of flight in which the flyer is airborne at a fixed position in space in still air.

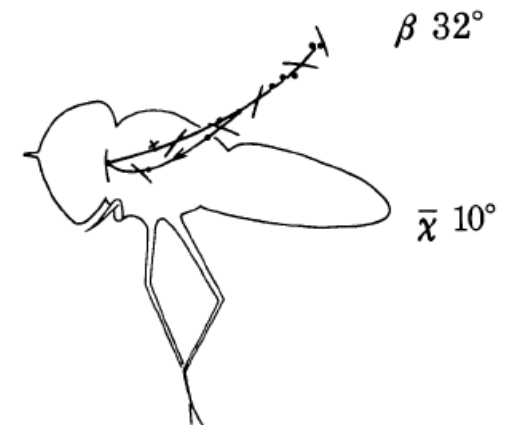
□ Two types of hovering may be distinguished:

- **Normal hovering:** as distinguished by the wings sweeping close to a horizontal plane. (Weis-Fogh 1973)
- **Inclined stroke plane hovering:** where the mean stroke plane is inclined at a significant angle to the horizontal.

□ Inclined stroke plane hovering is frequently used by insects when hovering with nearly horizontal posture.



**Horizontal mean stroke plane**



**Inclined mean stroke plane  
– hover fly. From Ellington  
(1984)**

## Hovering Flight (Contd.)

- ❑ A heuristic analysis shows that **Hovering** as a **free periodic state of flight** is **unstable**.
- ❑ Hence free hovering flight could only be achieved under some form of **active control**.
- ❑ To recall Dudley (2000)\*, even “**steady flight** (of insects) is perhaps best viewed as a sequence of consecutively unstable but controlled aerodynamic conditions; (where) compensatory course correction must continuously characterize flight with flapping wings.”
- ❑ This comment underscores the
  - **highly unstable and dynamic character** of insect flight and the
  - **need and ability of insects to continually control its wing kinematics** as part of the
  - **in-built reflexive response** of the insect locomotory system.
- ❑ The (biologically motivated) flight control modality or regime actually used by insects is not well known. A PID-type control algorithm is used to achieve free hovering flight that are broadly consistent with established observations.

\*Dudley, R (2000) Chapter Five – Stability, maneuverability and maximum flight performance. *The Biomechanics of Insect Flight: Form, Function, Evolution*. Princeton, Princeton University Press.



# The model fruit fly

- Our first flapping-wing flyer is modelled after the small fruit fly *Drosophila melanogaster*.
- The geometric model of the flyer was constructed approximately from photographic images of the insect and wings.

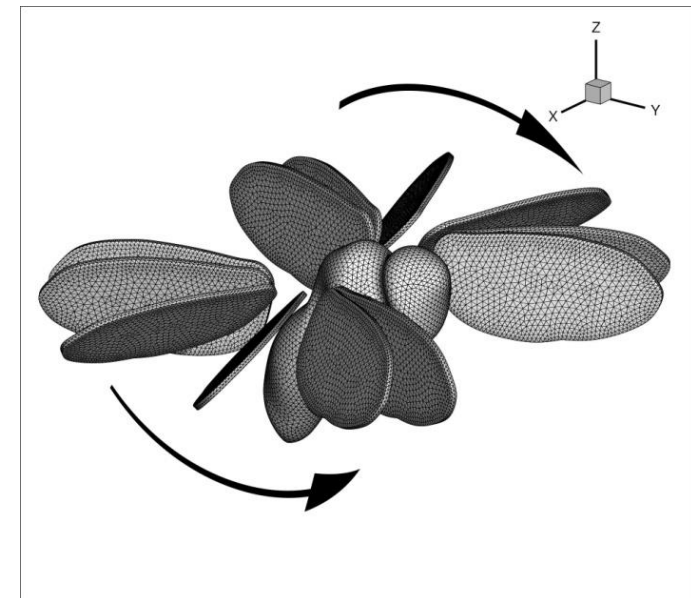
## Morphological data from Fry et al. (2005)\*

Body length	$L$	2.78 mm
Wing length	$R$	2.39 mm
Mean wing chord	$\bar{c}$	0.874 mm
Stroke angle	$\Phi$	2.44 rad (140°)
Wing-beat frequency	$f$	218 Hz
Weight	$W$	0.96 mg

$$\text{Nominal Re} = \frac{\bar{c} \cdot U_{ref}}{\nu} = \frac{\bar{c} \cdot (2\Phi f R)}{\nu} = 127$$

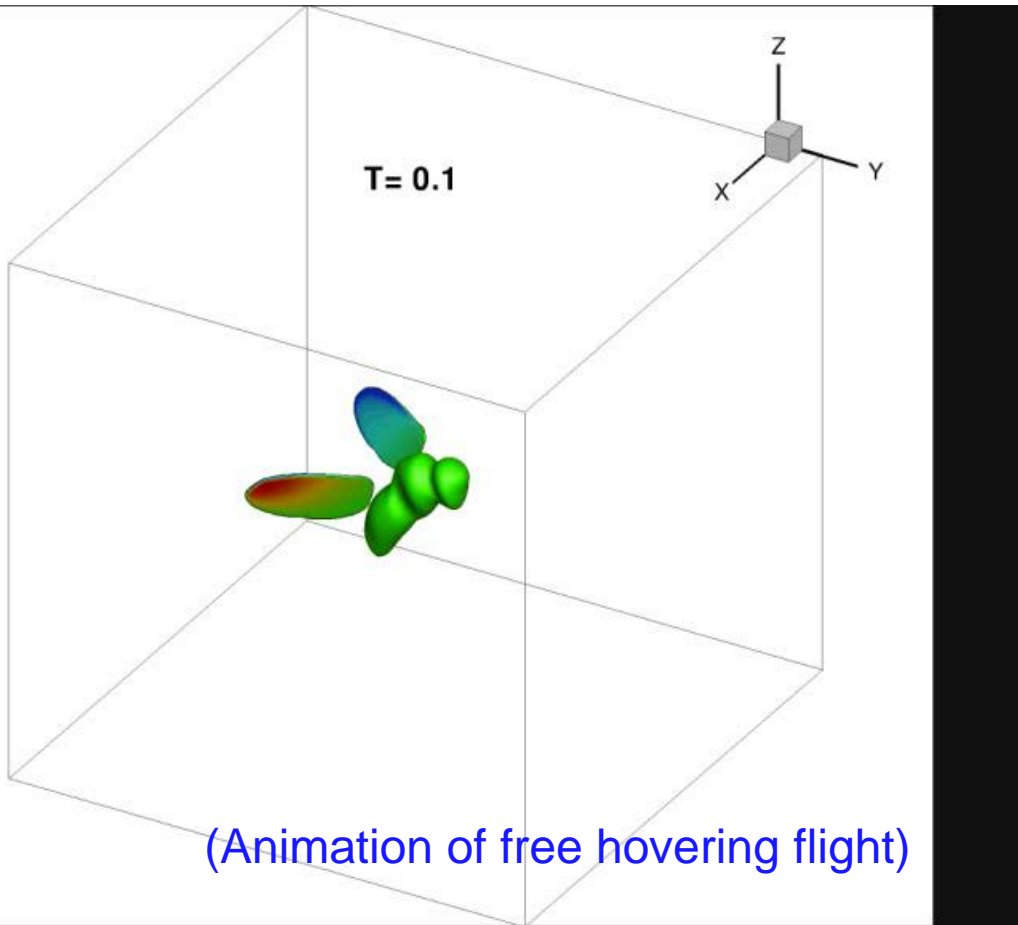
where  $\nu = 1.5 \times 10^{-5} \text{ m}^2\text{s}^{-1}$ .

\*Fry et al. (2005) J. Exp Biol. 208 2303-2318.

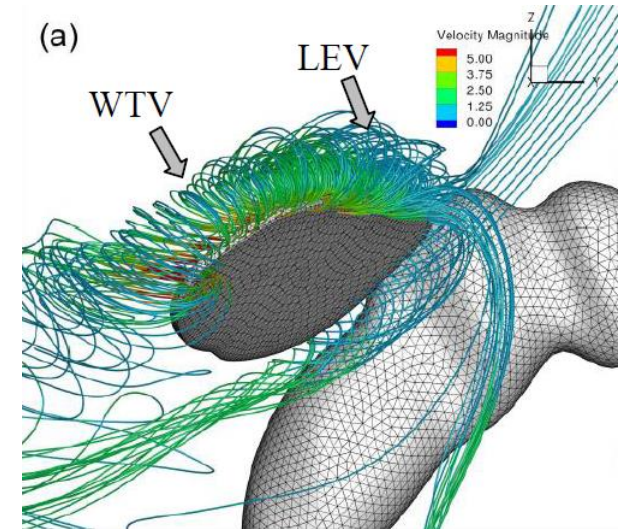


**Geometric model with smooth rigid wings of thickness  $0.02R$ .**

# Normal hovering flight – model fruit fly

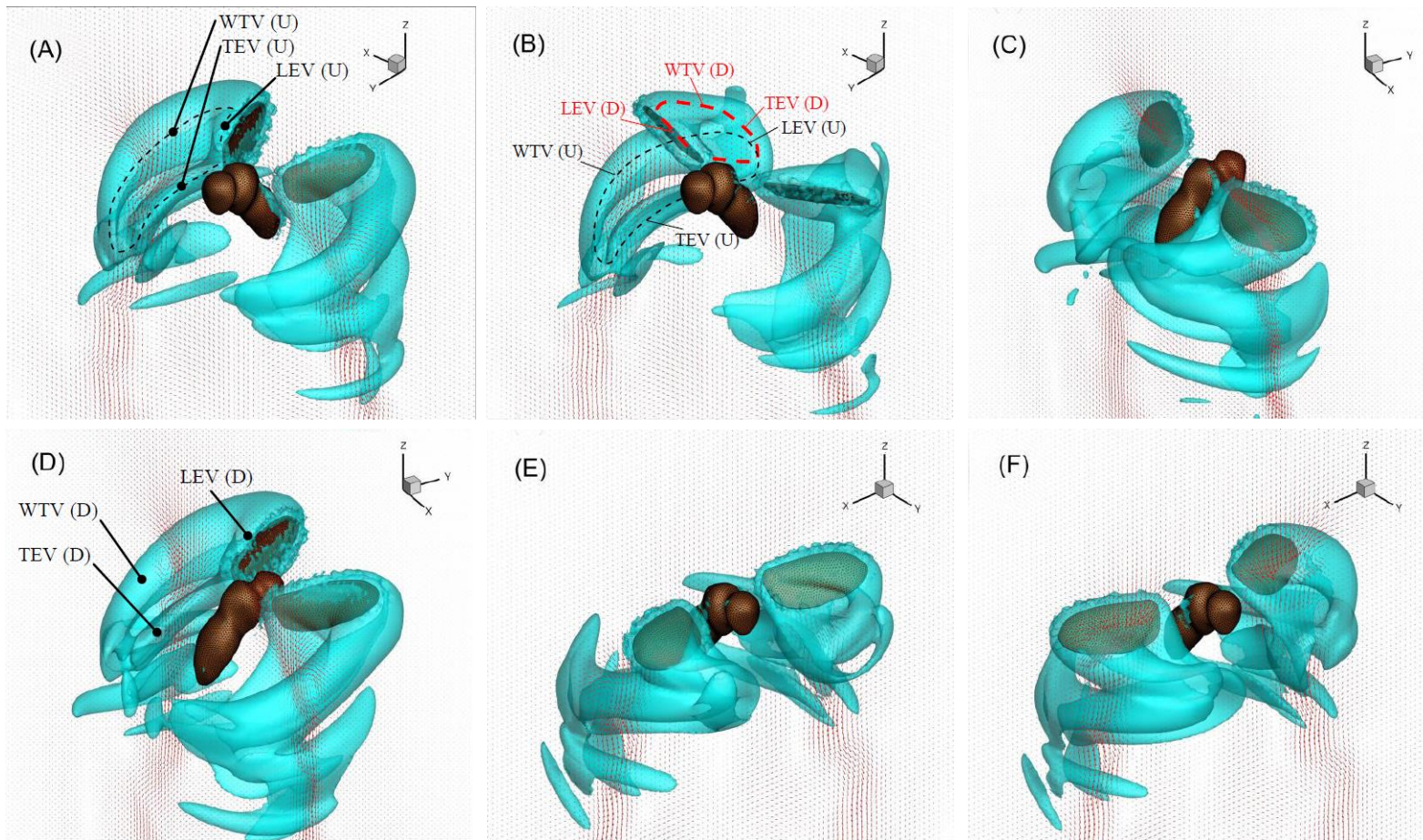


Normal (free) hovering in time



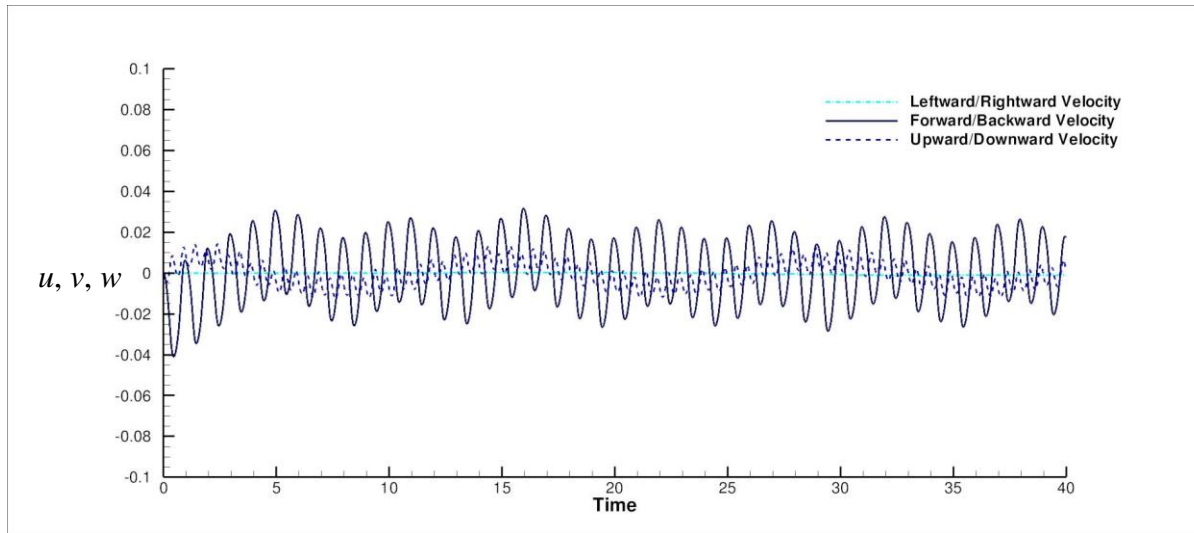
Typical LEV and WTV visualized by stream traces around the leading edge and wing tip regions in normal hovering.

## (Normal hovering-model fruit fly - Contd.)



Iso-vorticity surfaces around the model fruit fly at six consecutive time instances (A)-(F) ( $t = 10.0, 10.2, 10.3, 10.5, 10.7, 10.8$ ) of a wing cycle during normal hovering. Velocity fields in a lateral plane cutting across the vortex system. The (U) and (D) denote the upstroke and downstroke respectively.

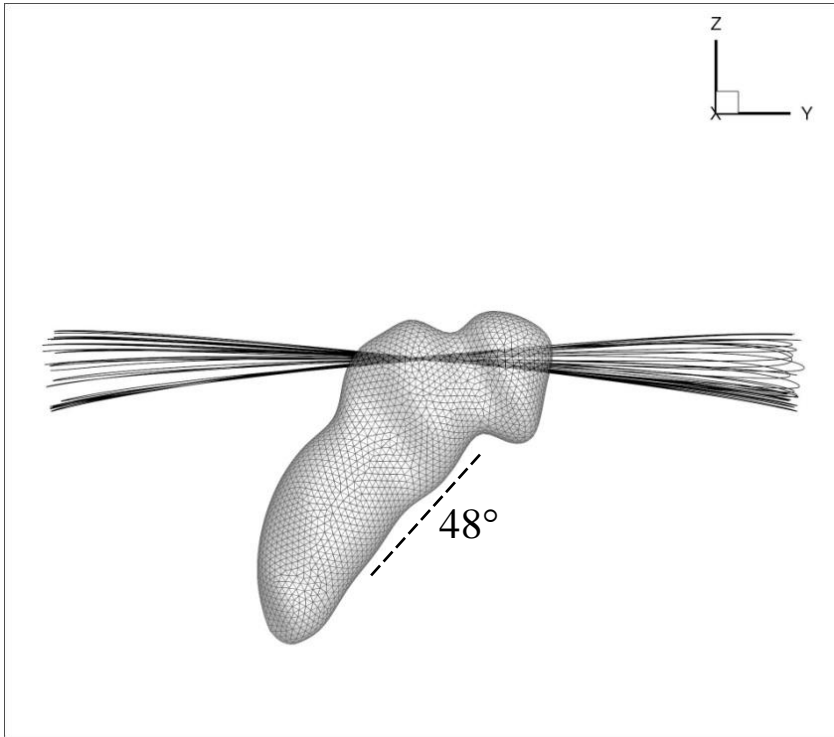
## (Normal hovering-model fruit fly - Contd.)



**Translation velocity  
fluctuations of the  
centre of mass /  $R_f$  .**



# (Normal hovering-model fruit fly - Contd.)



Projected wing-tip trajectory on the  $(y,z)$ -plane and approximate mean hovering posture of body.

The Centre of Mass position

$$\mathbf{x} = \bar{\mathbf{x}} + \Delta\mathbf{x} \approx \mathbf{0} + \mathbf{0.03}$$

The hovering stroke plane is approximately horizontal,

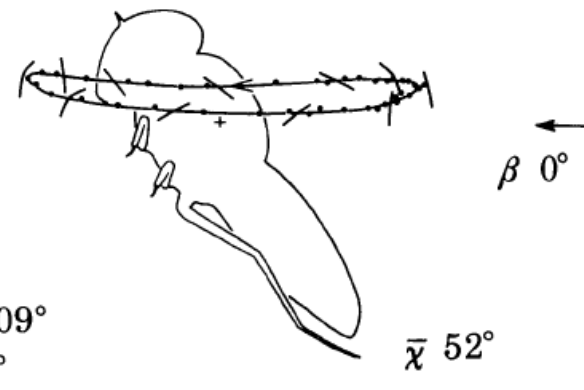
$$\beta = \bar{\beta} \pm \Delta\beta \approx 0 \pm 5^\circ$$

The body pitch angle from the horizontal

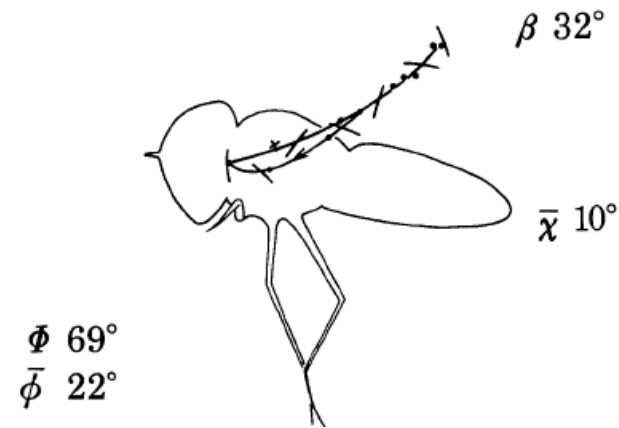
$$\chi = \bar{\chi} \pm \Delta\chi \approx 48 \pm 1.5^\circ$$

Ellington (1984)'s example:

Mean positional stroke angle  $\bar{\gamma} \approx 2^\circ$ .



# Inclined body, inclined stroke plane hovering



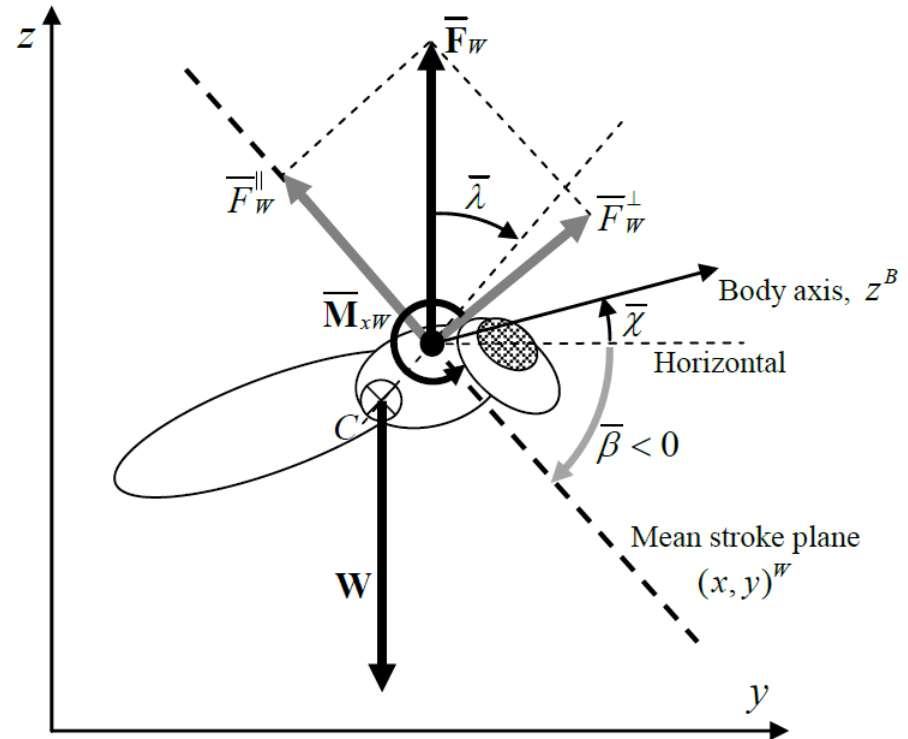
□ Why the need for inclined stroke plane during hovering?

- Insects frequently hover with a nearly horizontal posture when foraging over flowers.
- The wings then sweep more towards the rear to generate the needed pitch-down moment. If the sweep/stroke plane is horizontal and body are both horizontal, this may cause the wings to hit the body causing possible damage to the wings. To avoid this, the insects sweep its wings at an inclined plane (such as shown above).
- There may also be other reasons for using inclined stroke plane.

**Inclined mean stroke plane – hover fly. From Ellington (1984).**

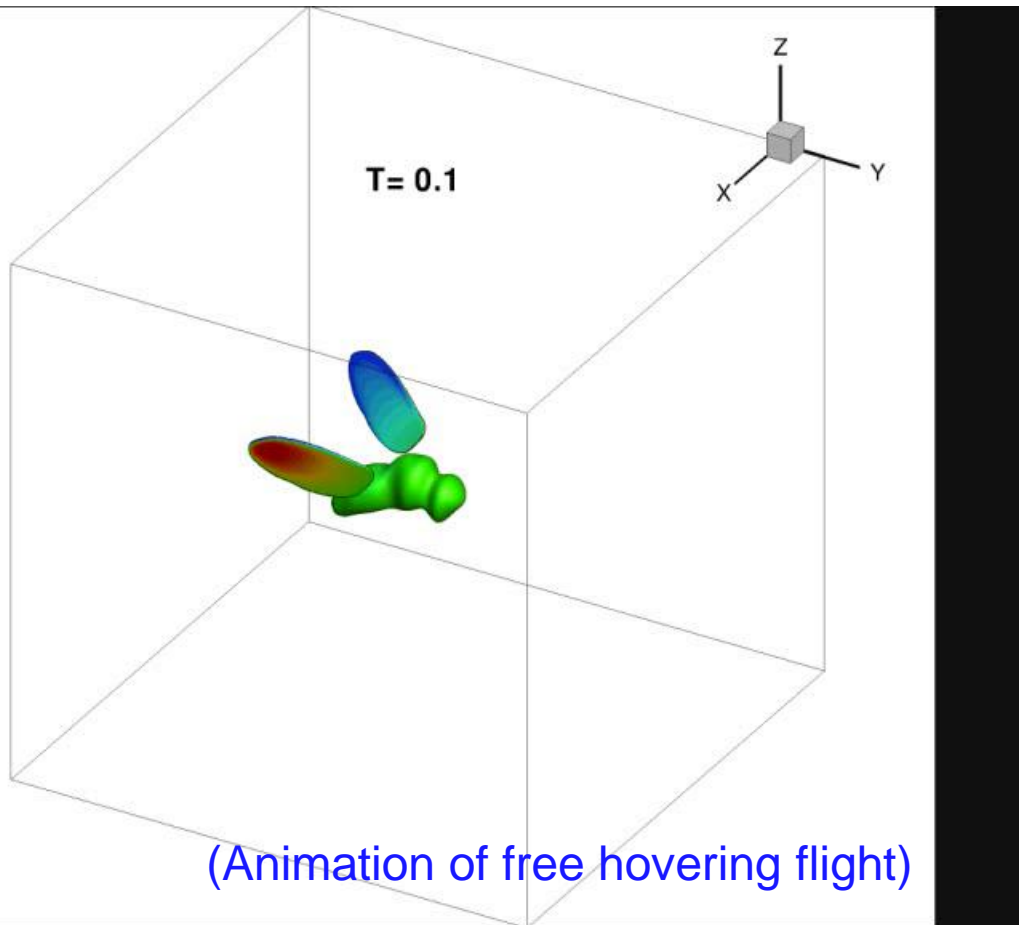
# Inclined stroke plane hovering

- The mean wing force  $\bar{\mathbf{F}}_w$  now has both a normal component  $\bar{F}_w^\perp$  and a significant tangential component  $\bar{F}_w^\parallel$  along the mean stroke plane.
- Phasic wing elevation / Stroke plane adjustment is now complemented by **non-symmetric** (inner) wing kinematics in the wing frame.

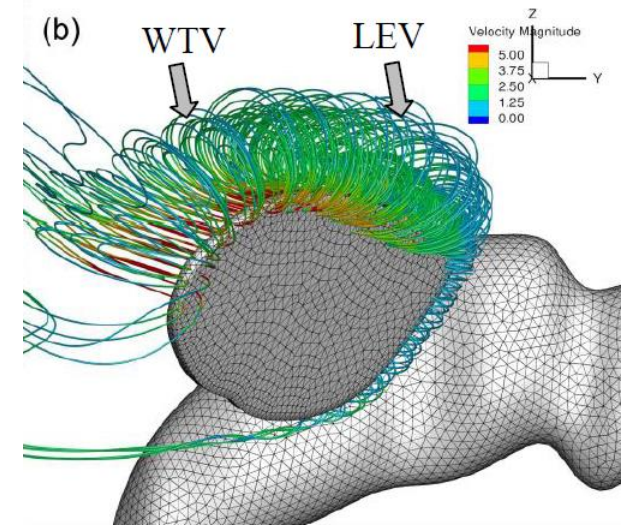


**Inclined-body hovering with highly inclined mean stroke plane. Non-symmetric inner wing kinematics generates a component of mean wing force along the stroke plane**

# Inclined-body hovering flight – model fruit fly



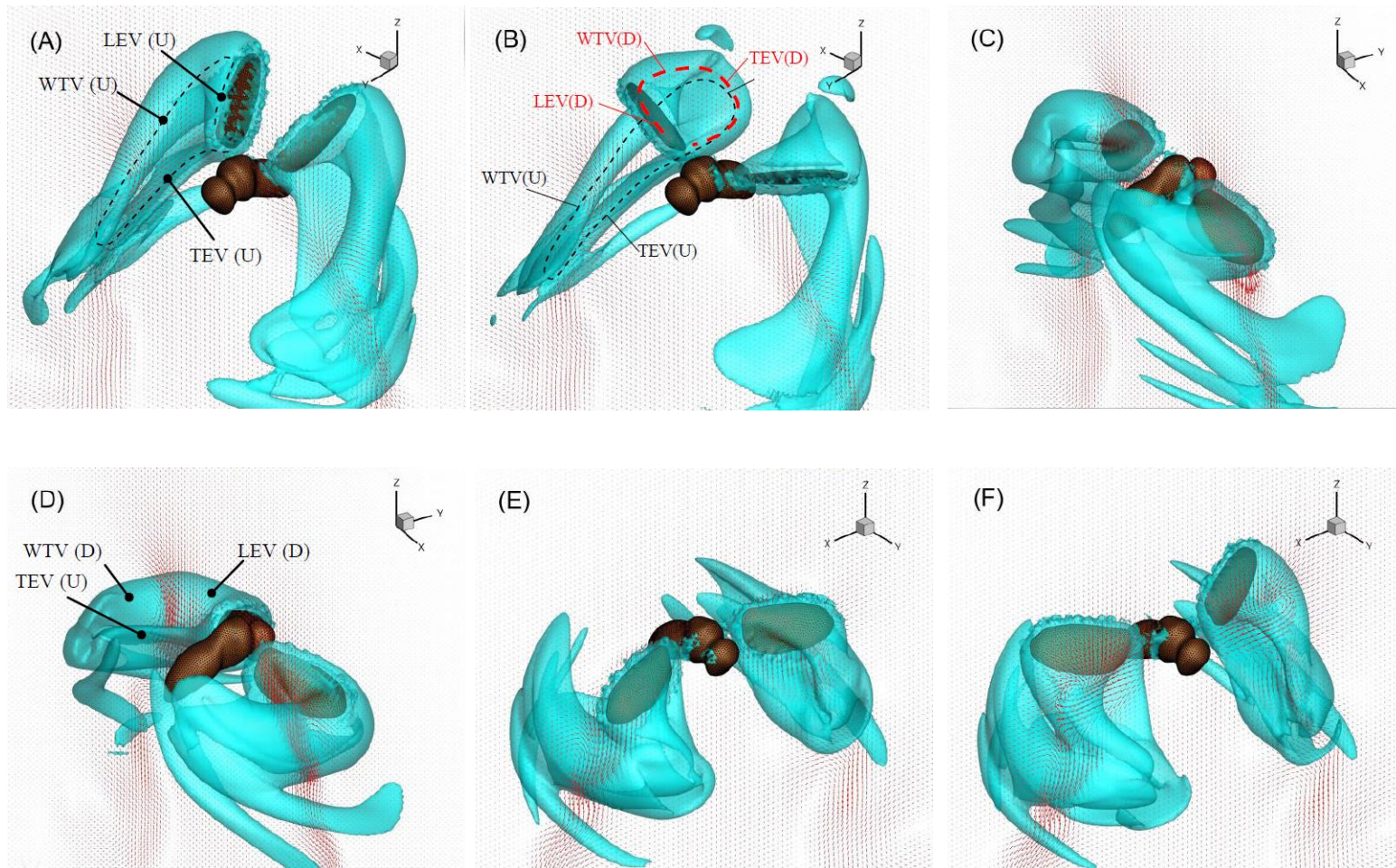
Inclined-body, inclined stroke-plane (free) hovering in time



LEV and WTV visualized by stream traces around the leading edge and wing tip regions in inclined stroke plane hovering.

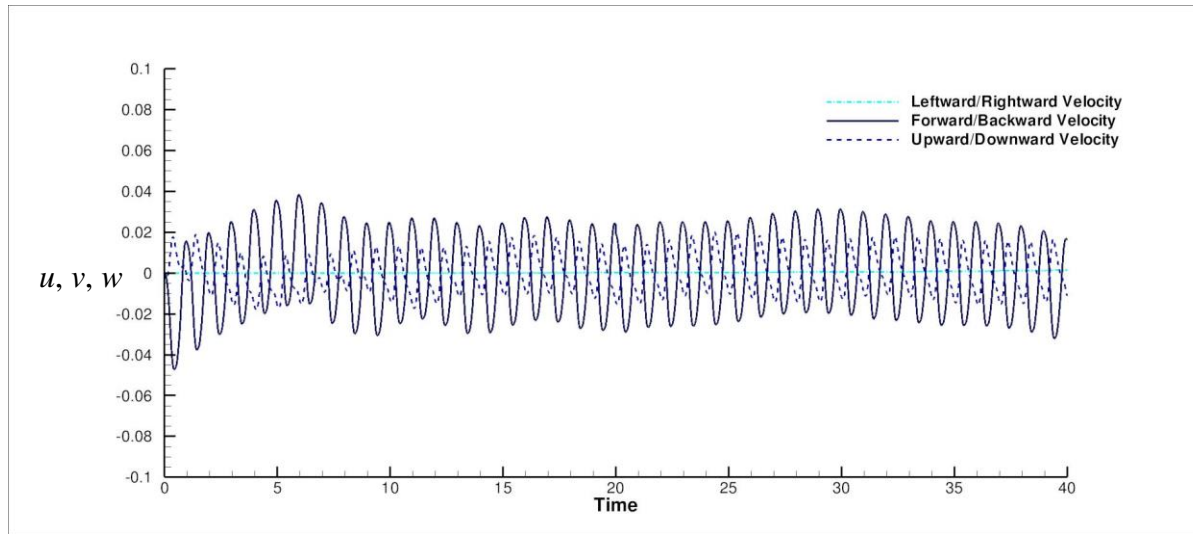


# Inclined-body hovering flight (Contd.)



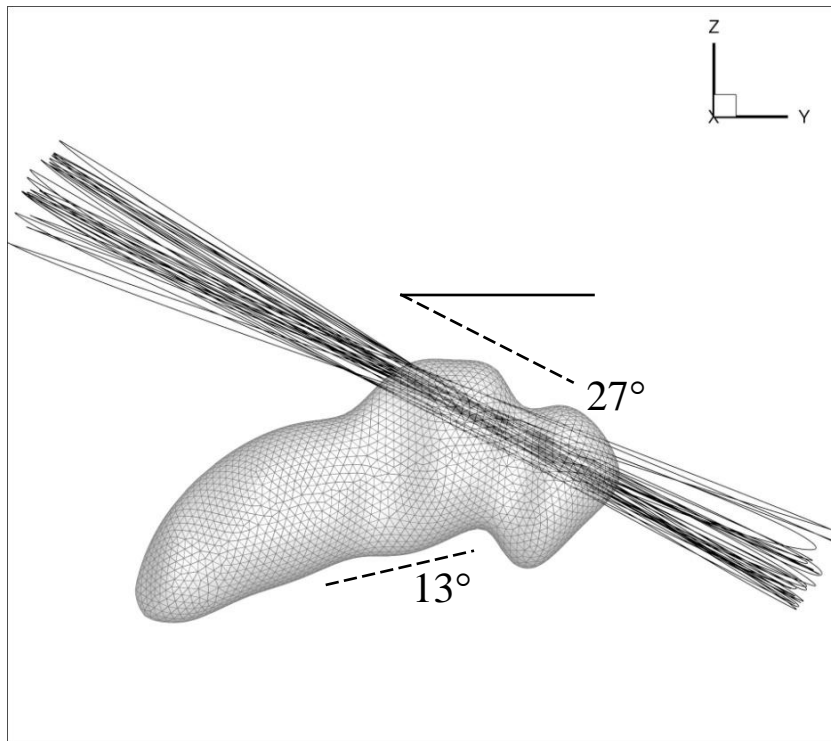
Iso-vorticity surfaces around the model fruit fly at six consecutive time instances (A)-(F) ( $t = 10.0, 10.2, 10.3, 10.5, 10.7, 10.8$ ) of a wing cycle during inclined stroke plane hovering. Velocity fields in a lateral plane cutting across the vortex system. The (U) and (D) denote the upstroke and downstroke respectively.

# Inclined-body hovering flight (Contd.)



**Translation velocity  
fluctuations of the  
centre of mass /  $R_f$  .**

# Inclined-body hovering flight (Contd.)



Projected wing-tip trajectory on the  $(y,z)$ -plane and approximate mean hovering posture of body.

The Centre of Mass position

$$\mathbf{x} = \bar{\mathbf{x}} + \Delta\mathbf{x} \approx \mathbf{0} + \mathbf{0.04}$$

The mean hovering stroke plane is approximately inclined with,

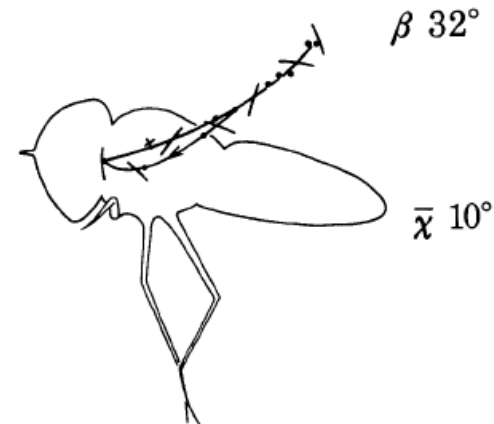
$$\beta = \bar{\beta} \pm \Delta\beta \approx 27 \pm 5^\circ$$

The body pitch angle from the horizontal

$$\chi = \bar{\chi} \pm \Delta\chi \approx 13 \pm 2.5^\circ$$

Ellington (1984)'s example:

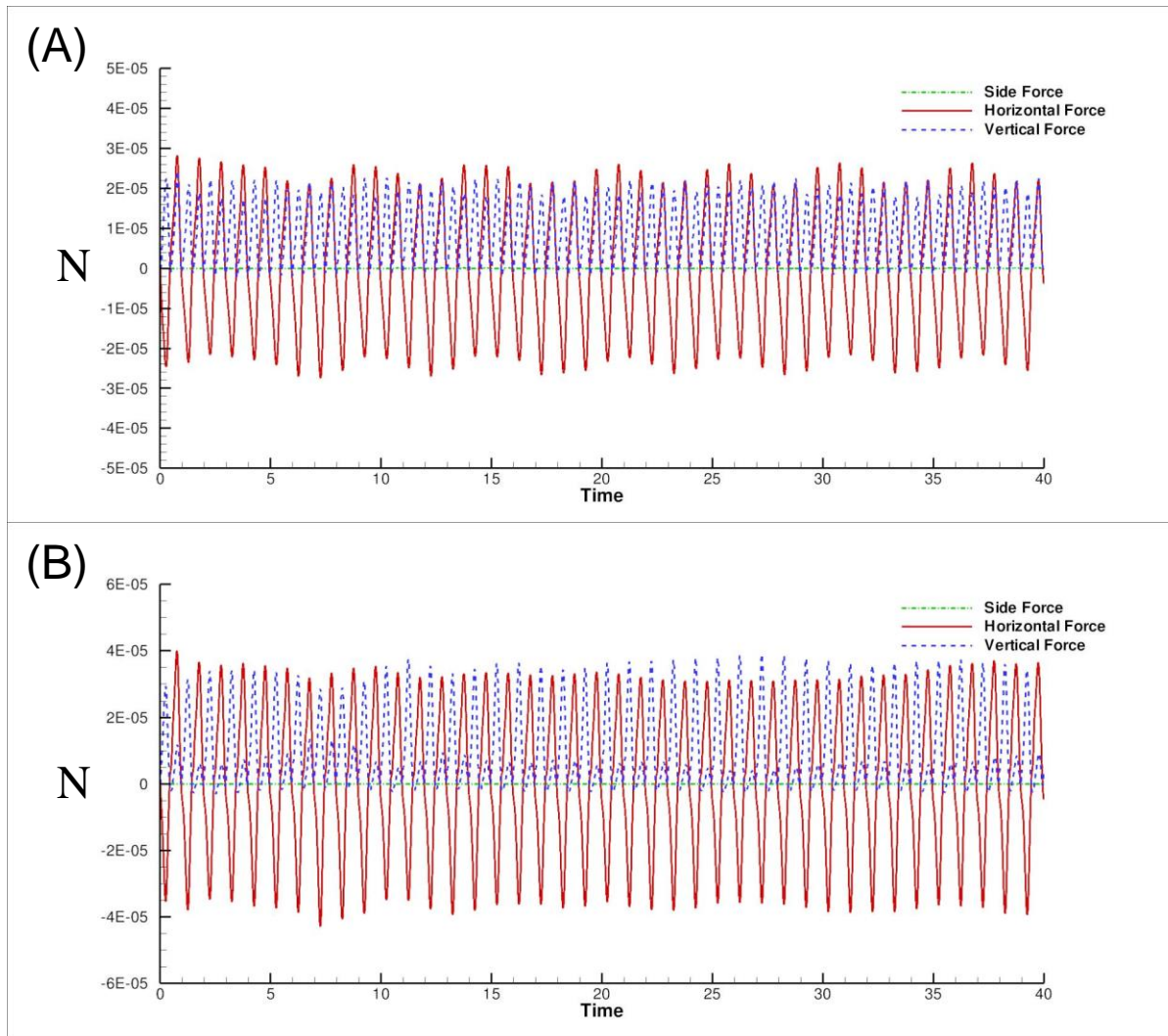
Mean positional stroke angle  $\bar{\gamma} \approx 5^\circ$ .



$$\begin{aligned} \phi & 69^\circ \\ \bar{\phi} & 22^\circ \end{aligned}$$



# Normal versus Inclined stroke plane hovering – Fruit fly



Peak Lift force in downstroke and upstroke are about the same magnitude  $> W = 0.94 \times 10^{-5}$  N.

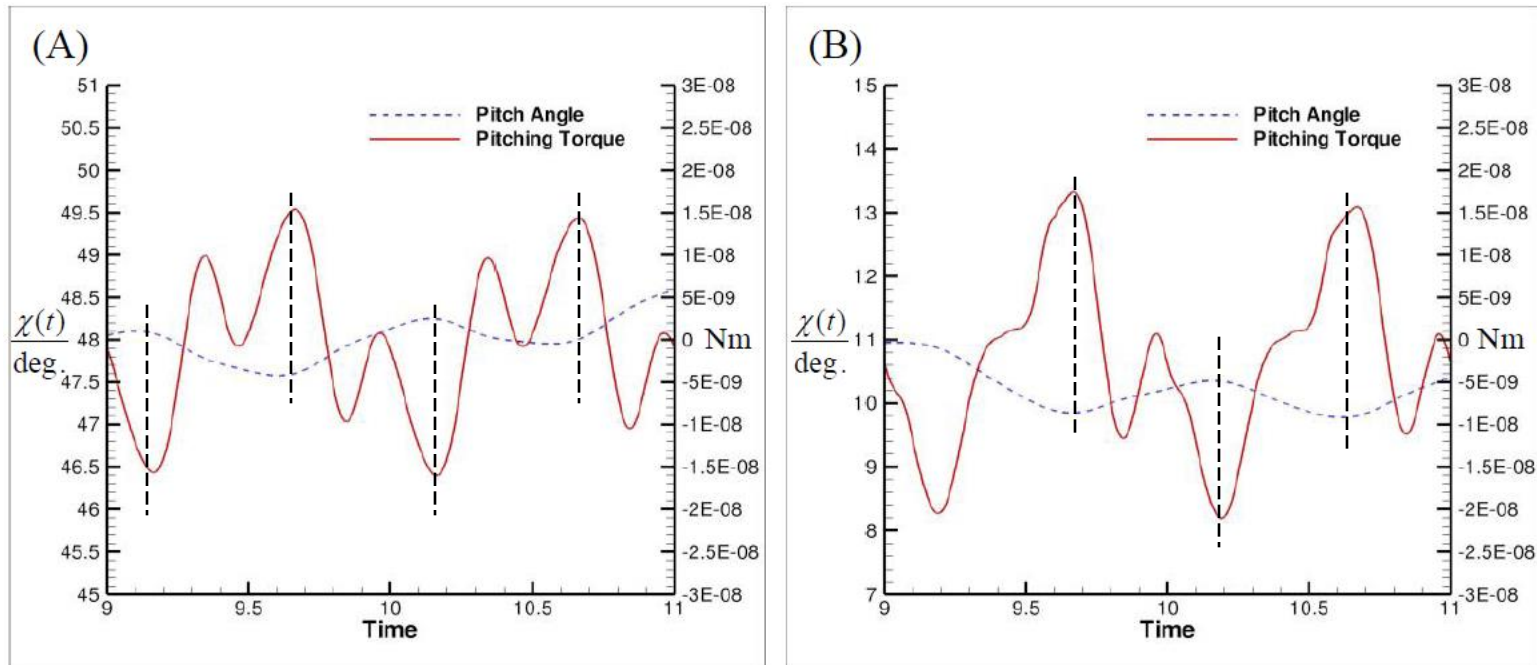
Downstroke and upstroke peak (and mean) lift are about 5:1 (mean stroke plane  $\beta \approx 27^\circ$ )

Ellington (1984)\*  
Drone fly: estimated 3.4:1 (mean  $\beta \approx 21^\circ$ ).  
The ratio increases rapidly with  $\beta$ .

History of computed vertical, horizontal and lateral/side forces over 40 flapping wing cycles for (A) normal hovering and (B) inclined-body hovering.

\**Phil. Trans. R. Soc. Lond. B* 1984  
305, 145-181.

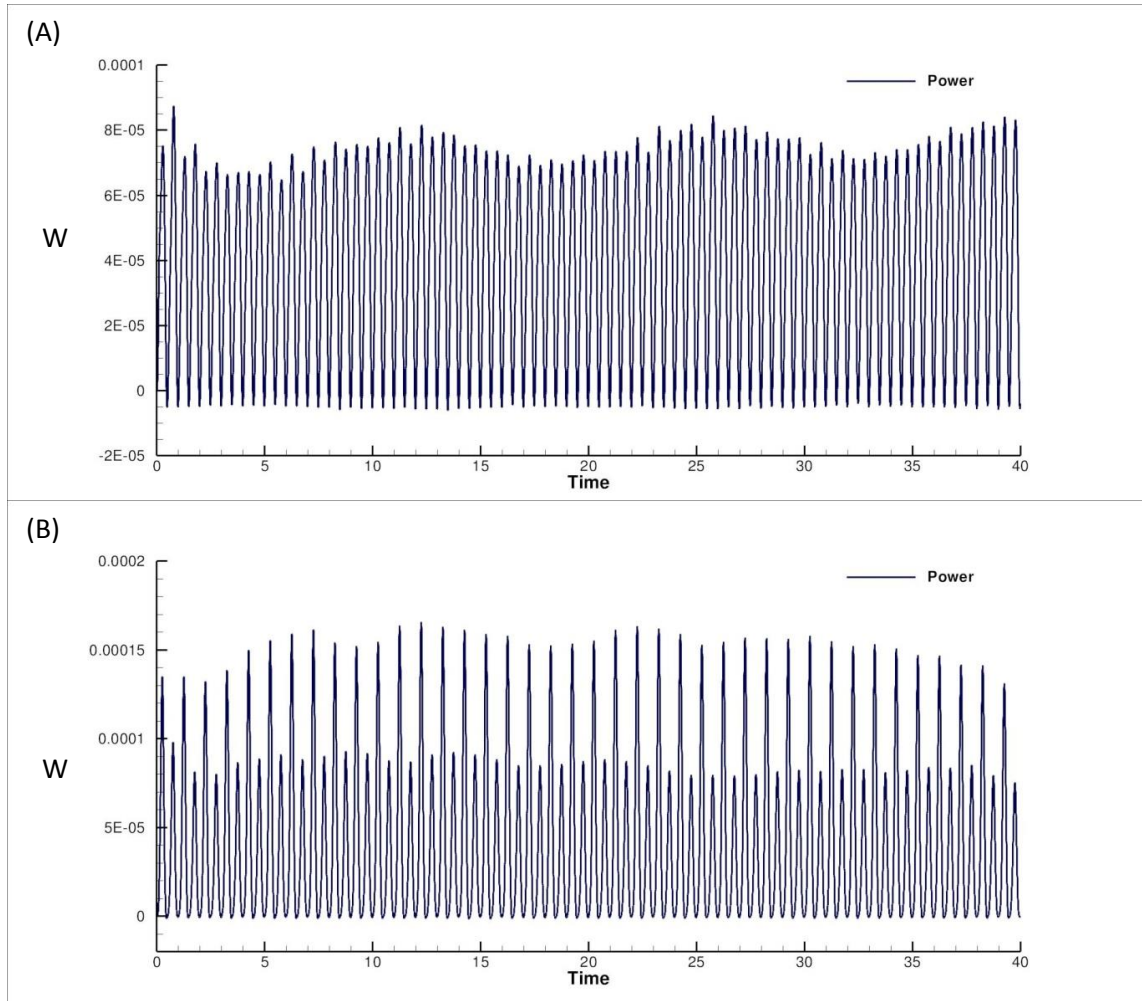
## Normal versus Inclined (Contd.)



**Body pitching angle  $\chi(t)$  versus aerodynamic pitching moment about the centre of mass in the 9<sup>th</sup> and 10<sup>th</sup> wing cycles for (A) normal hovering and (B) inclined stroke plane hovering.**

- Within a wing cycle, the local maximum and minimum pitch angles of the body occur near to the dorsal and ventral ends of the stroke ( $\approx +30$ - $45^\circ$  for normal and  $\approx +40$ - $60^\circ$  for inclined-body hovering behind the start of stroke), respectively. These are in good agreement with the observations of Ellington (1984c).

## Normal versus Inclined (Contd.)



*Specific aerodynamic power* ( aerodynamics power per unit of body weight) is  $4.07 \text{ WN}^{-1}$  for normal hovering ( $\text{Re} \approx 150$ )

Estimates:

Fry et al. (2005) hovering fruit fly  
 $\text{Re} = 153$ ;  $3.0 \text{ WN}^{-1}$   $\sigma = 0.83$ .

Weis-Fogh (1973) *Diptera*, 2-wing *Aedes aegypti*, normal hovering  $\text{Re} = 170$ ;  $3.33 \text{ WN}^{-1}$ .

*Specific aerodynamic power* is  $6.35 \text{ WN}^{-1}$  for the inclined stroke plane hovering case.

**The history of aerodynamic power over 40 flapping wing cycles for (A) normal hovering and (B) inclined-body hovering (in Watt).**

# The model hawkmoth (*Manduca sexta*)

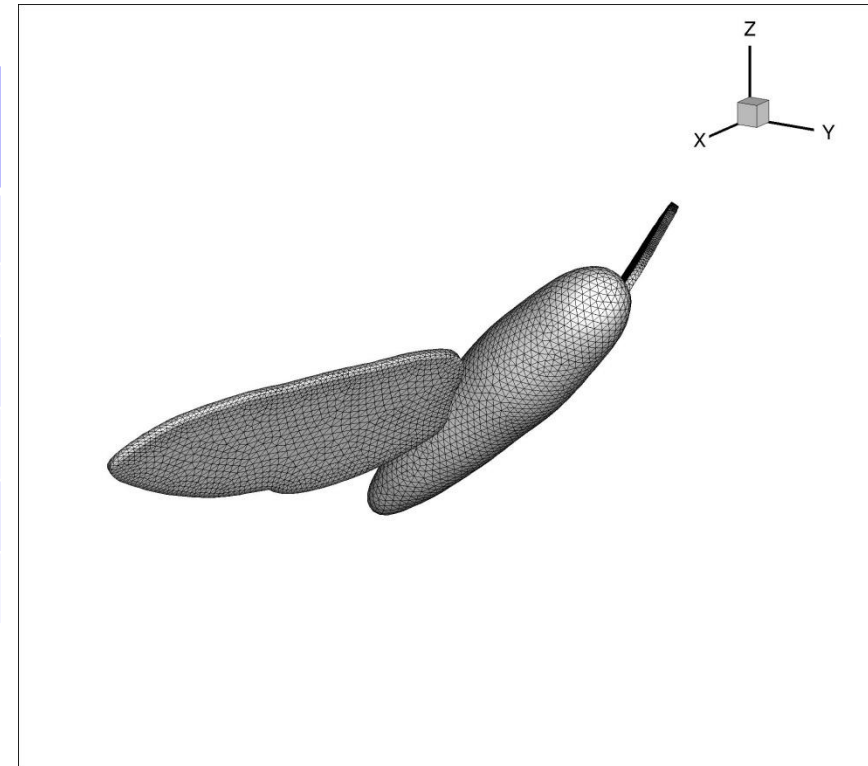
- This a much larger insect than the Fruit Fly.

## Morphological data from Hedrick et al. (2006)\*

Body length	$L$	46.6 mm
Wing length	$R$	53 mm
Mean wing chord	$\bar{c}$	18.7 mm
Stroke angle	$\Phi$	2.0 rad (114°)
Wing-beat frequency	$f$	25 Hz
Weight	$W$	1.969 g

$$\text{Nominal } \text{Re} = \frac{\bar{c} \cdot U_{ref}}{\nu} = \frac{\bar{c} \cdot (2\Phi f R)}{\nu} \approx 6,600$$

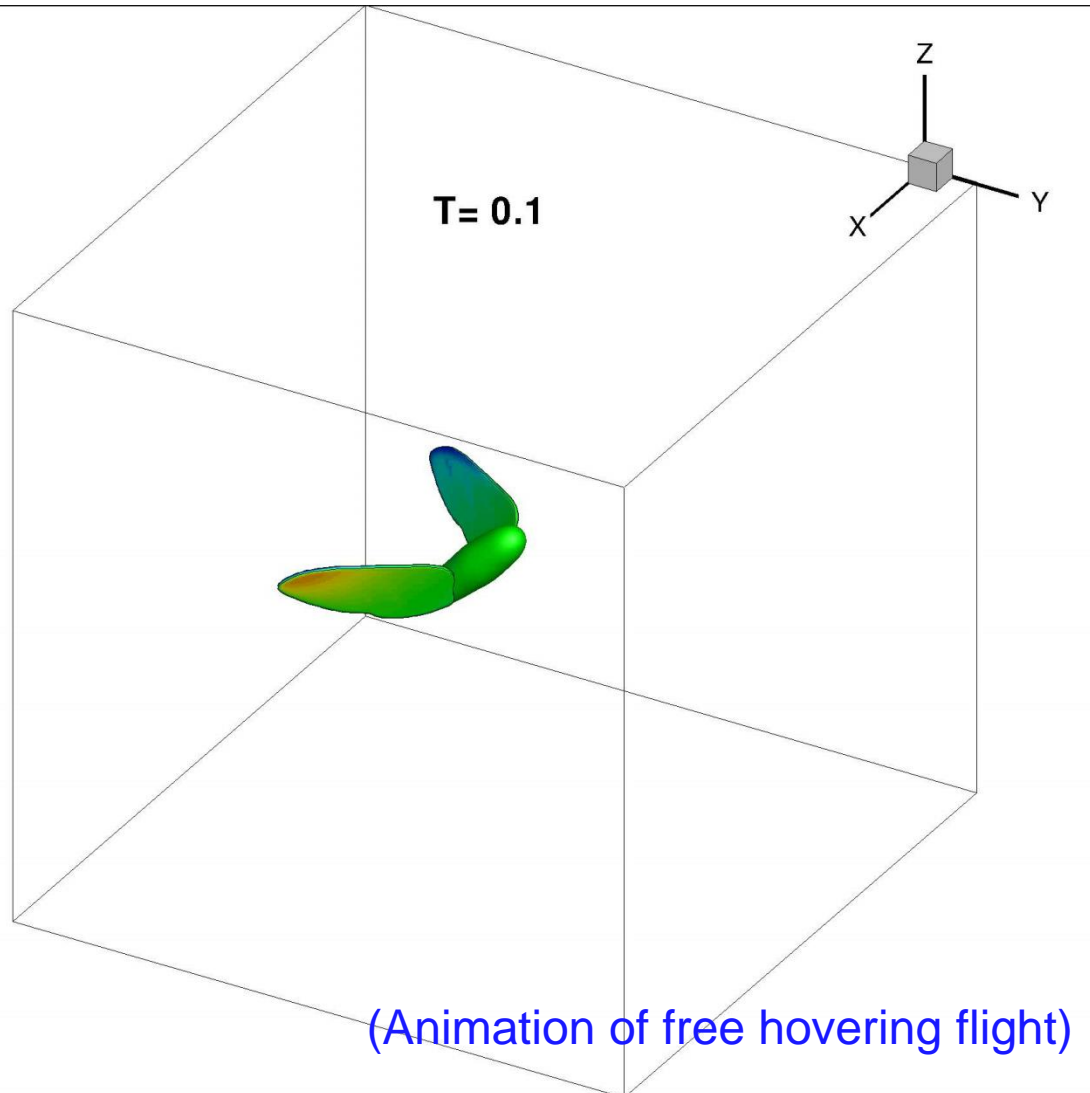
where  $\nu = 1.5 \times 10^{-5} \text{ m}^2\text{s}^{-1}$ .



**Geometric model with smooth rigid wings of thickness  $0.02R$ .**

\*Hedrick et al. (2006) J. Exp Biol. **209**, 3114-3130.

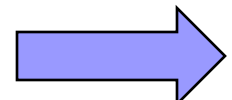
# Model hawkmoth (Contd.)



Normal (free) hovering of model Hawkmoth.

**Hovering Hawkmoth at a flower (from Youtube)**

<http://www.youtube.com/watch?v=ECipm4lzfQ>





## Model hawkmoth (Contd.)

Over 40 cycles

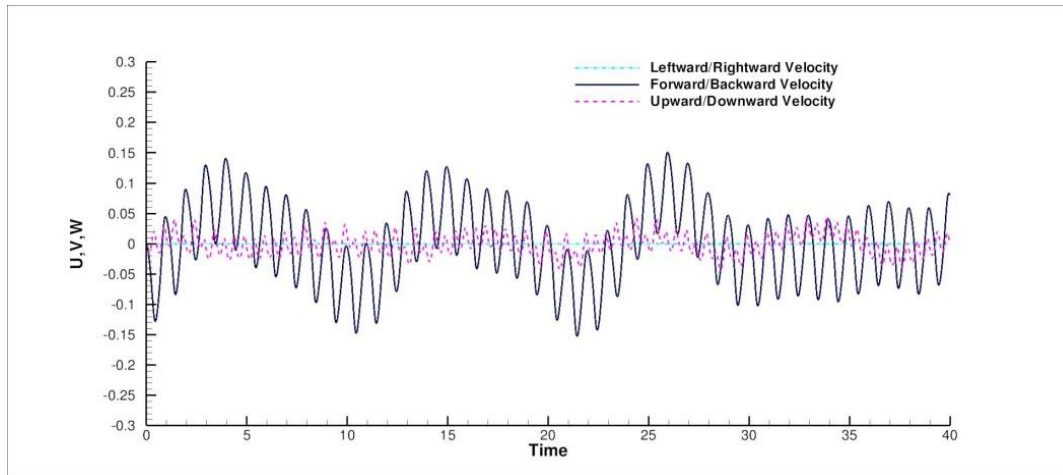
The Centre of Mass position:  $\mathbf{x} = \bar{\mathbf{x}} + \Delta\mathbf{x} \approx \mathbf{0} + \mathbf{0.1}$

The hovering stroke plane angle is approximately:  $\beta = \bar{\beta} \pm \Delta\beta \approx 6 \pm 7^\circ$

The body pitch angle from the horizontal:  $\chi = \bar{\chi} \pm \Delta\chi \approx 42 \pm 7^\circ$

Mean positional stroke angle:  $\bar{\gamma} \approx 10^\circ$ .

# Model hawkmoth – normal hovering (Contd.)



Variation of velocity of CoM with time.

Over 40 wing cycles

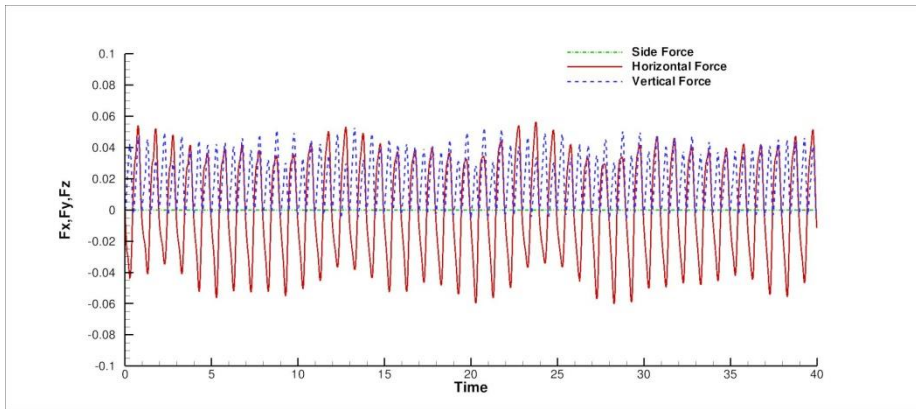
The Centre of Mass position:  $\mathbf{x} = \bar{\mathbf{x}} + \Delta\mathbf{x} \approx \mathbf{0} + \mathbf{0.1}$

The hovering stroke plane angle is approximately:  $\beta = \bar{\beta} \pm \Delta\beta \approx 6 \pm 7^\circ$

The body pitch angle from the horizontal:  $\chi = \bar{\chi} \pm \Delta\chi \approx 42 \pm 7^\circ$

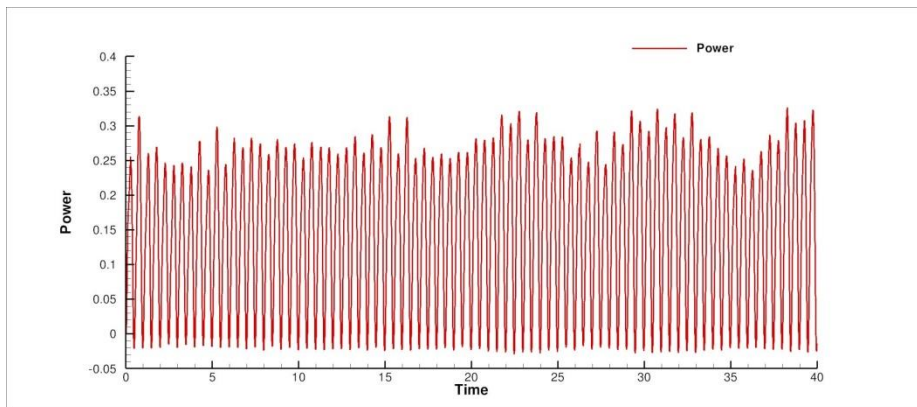
Mean positional stroke angle:  $\bar{\gamma} \approx 10^\circ$ .

# Hawkmoth – force, moment and power



Variation of forces (N) with time.

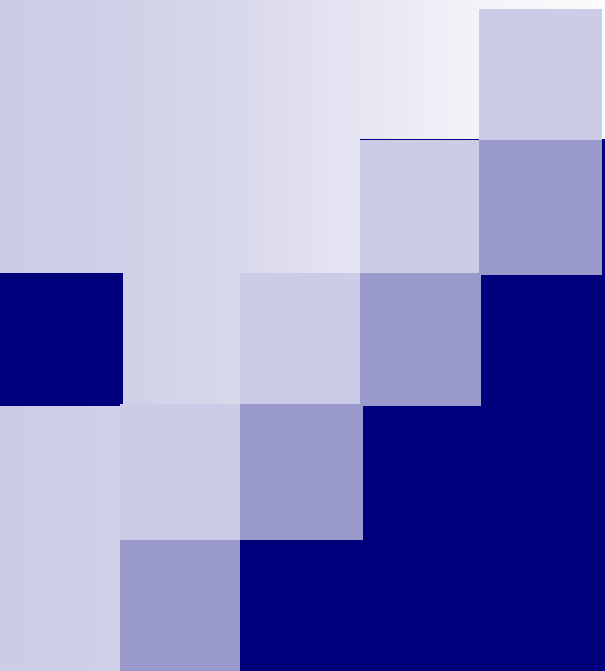
Flyer weight = 0.0193N.



Variation of aerodynamic power (W).

*Specific* aerodynamic power (aerodynamics power per unit of body weight)  $\approx \underline{5.7 \text{ WN}^{-1}}$ .

Overall, they display traits of normal hovering with relatively symmetric down and upstroke lift force and power.



# Rectilinear Free Flight

# Rectilinear free flight – Fruit fly

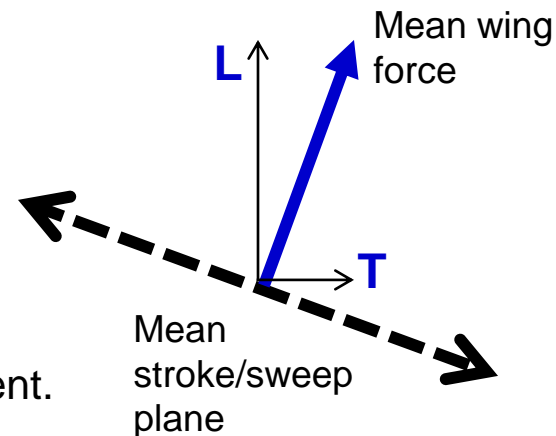
- Rectilinear flight of fruit fly is generated here by a combination of
  - Symmetric sinusoidal inner wing kinematics (which produces a wing force normal to the stroke plane):

$$\phi(t) = -\frac{7\pi}{18}\cos(2\pi t)$$

$$\theta(t) = 0$$

$$\psi(t) = \frac{\pi}{2} - \frac{\pi}{4}\sin(2\pi t)$$

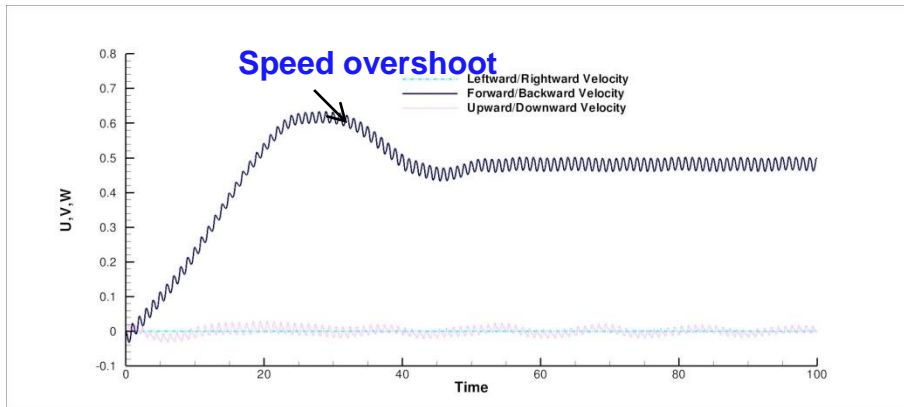
- Phasic wing elevation / stroke plane adjustment.



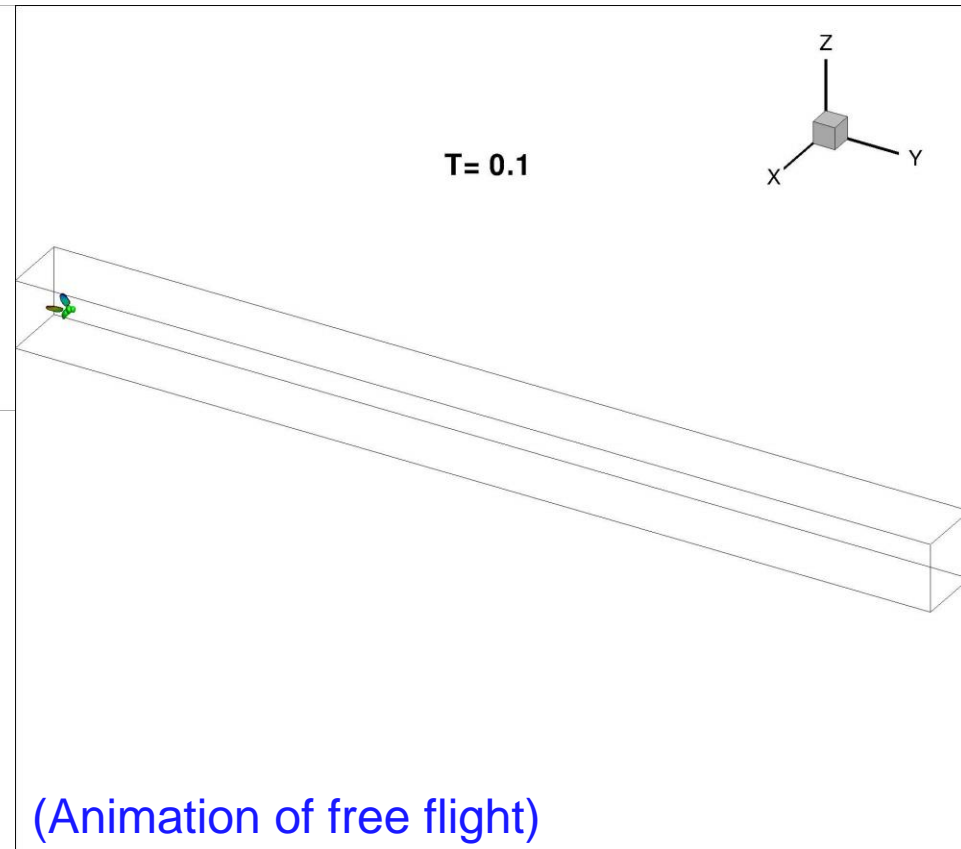
- Forward flight is realized by when phasic wing elevation is applied to bias the mean stroke plane angle forward.

# Forward Flight

Acceleration and forward flight at 30 cm/s (with NO roll-yaw)

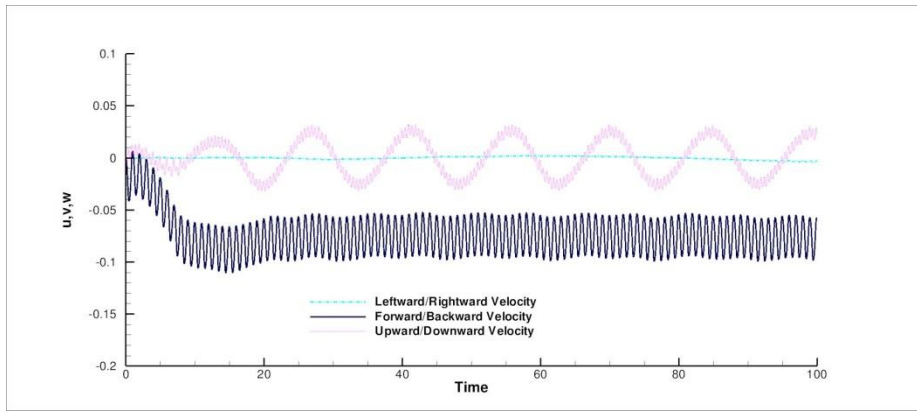


Velocity  $u, v, w$

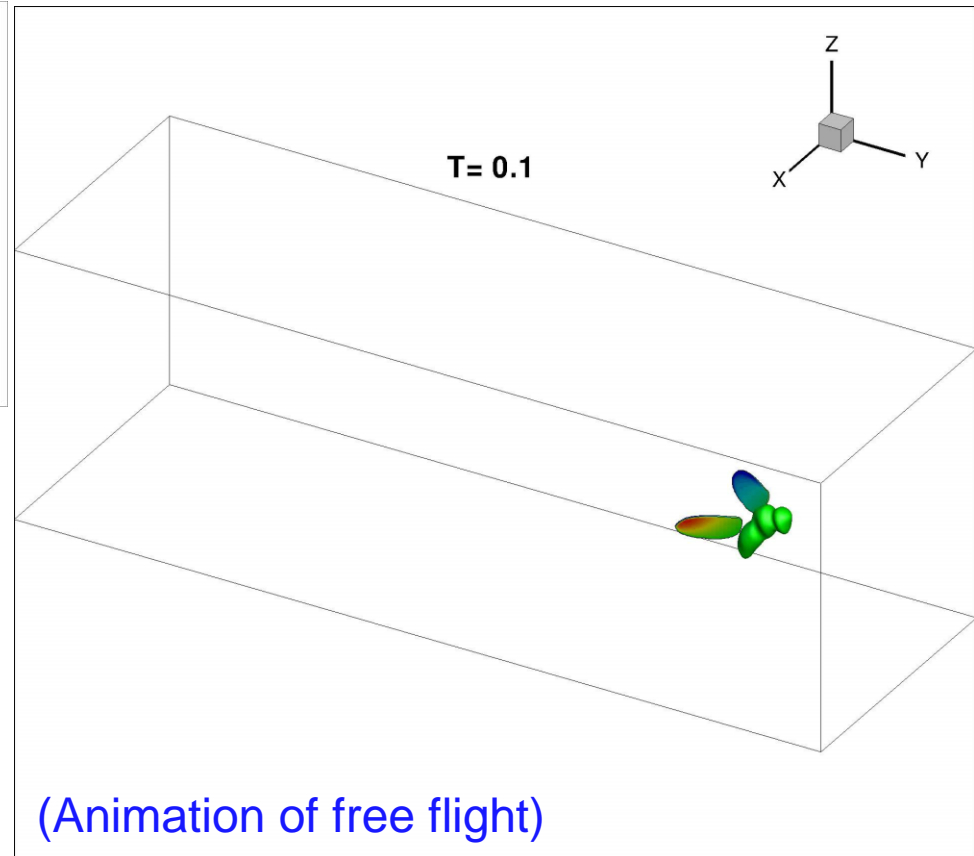


# Backward flight

Backward flight at  $-5$  cm/s (with roll-yaw)

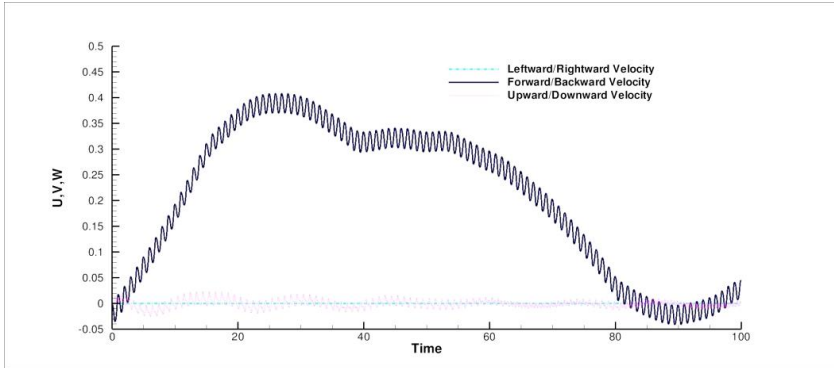


Velocity  $u, v, w$

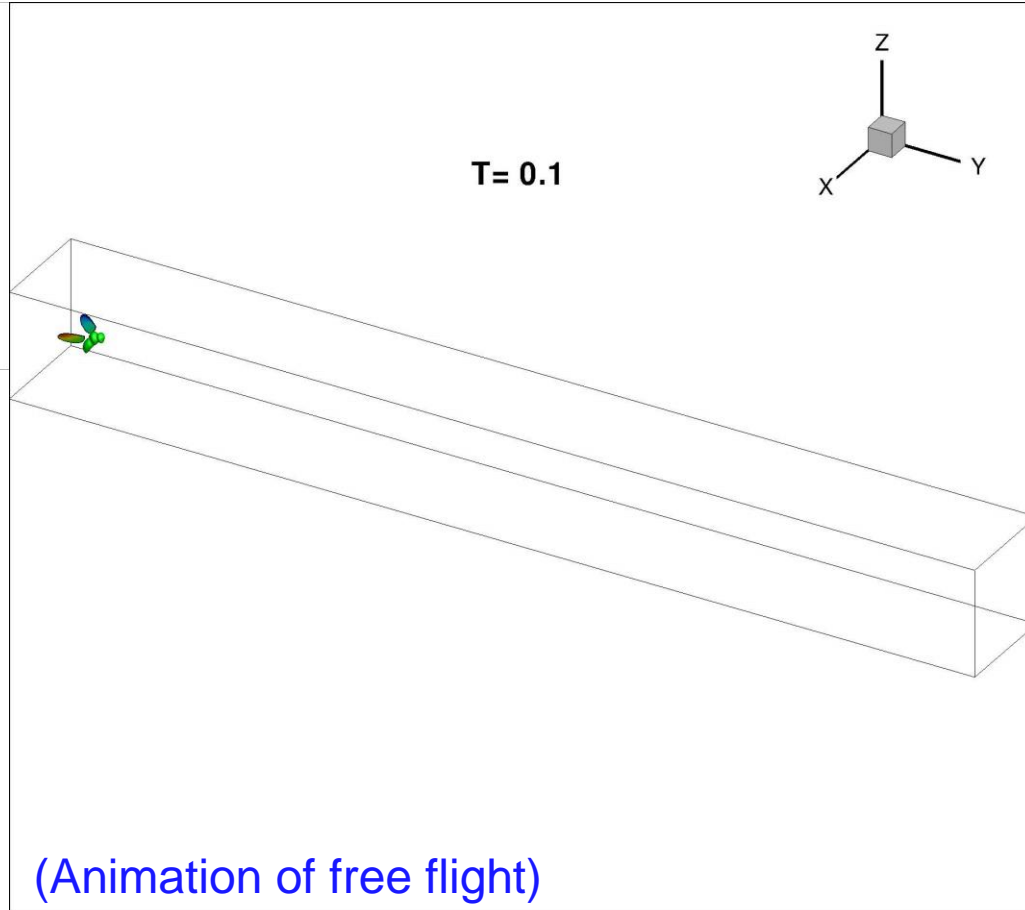


(Animation of free flight)

# Accelerating to 20 cm/s and decelerating to a hovering state (no roll-yaw)

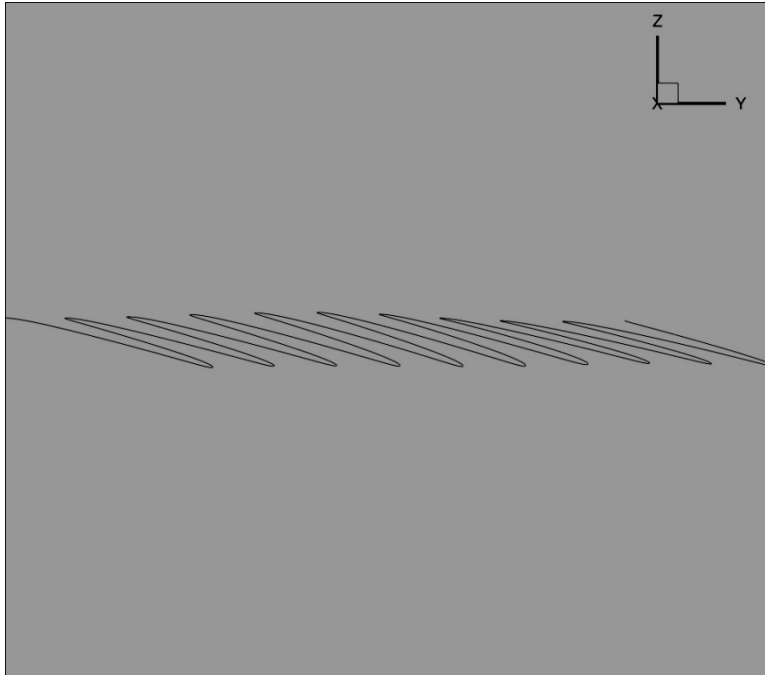


Velocity u, v, w



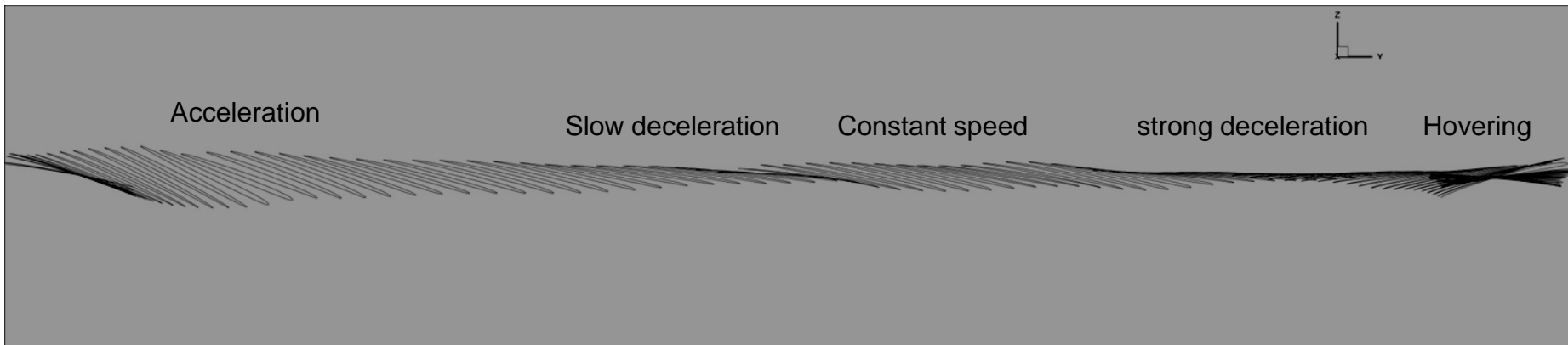


# Wing-tip trajectories



Wing-tip trajectory at the 70-80 cycles at 40 cm/s forward flight.

Wing-tip trajectory for acceleration – deceleration – hovering flight



# Conclusions of the free hovering and rectilinear flight study

- ❑ Hovering as a free periodic state of flight is unstable in the mean to long-time scale disturbances, and hence unstable.
- ❑ Sustained free hovering is a quasi-steady state that requires active control, especially in the physical environment, where disturbances in air flow abound.
- ❑ Free hovering with *horizontal* (normal) and *inclined* stroke planes were demonstrated numerically, using a rudimentary control system. The focus is on longitudinal stability, since no systematic roll-yaw control is implemented.
- ❑ Free rectilinear forward flight, backward flight and accelerating-to-decelerating-hovering flight have been demonstrated.
- ❑ The dynamical results obtained were in good overall agreement with published data and analyses.



*End*  
*Thank You for your*  
*Attention*



# Inner wing kinematics

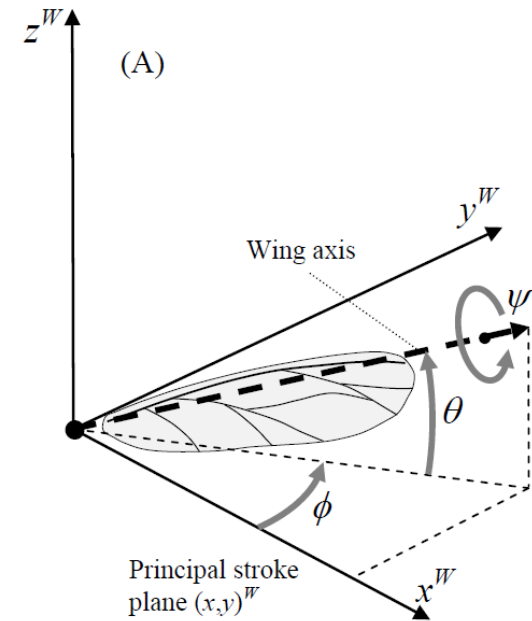
The wing kinematics in the wing frame:

$$\phi(t) = -\frac{7\pi}{18}\cos(2\pi t)$$

$$\theta(t) = 0$$

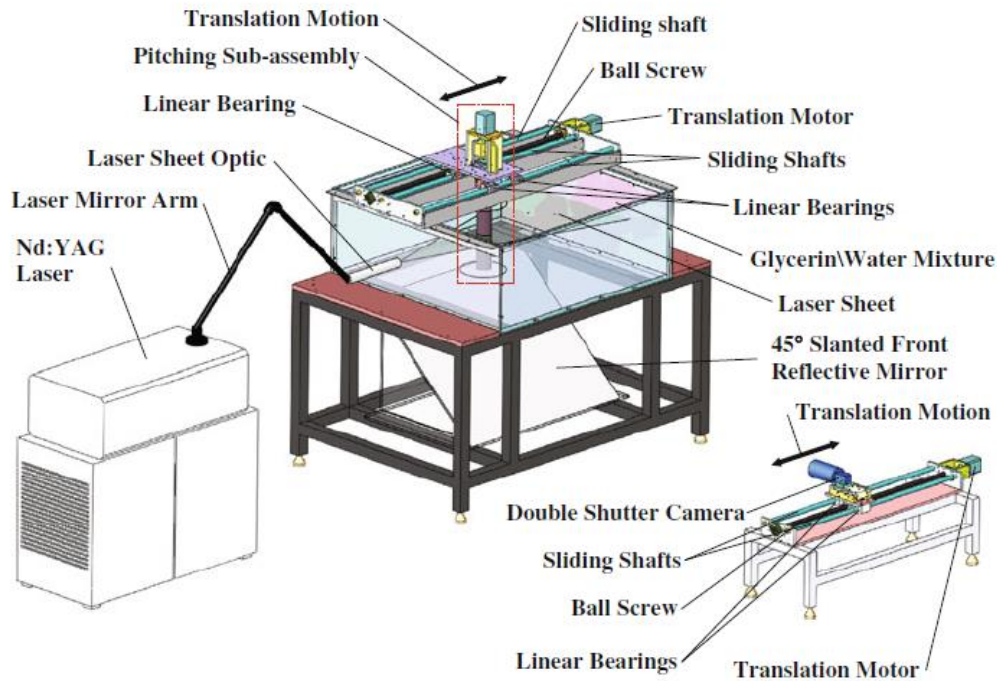
$$\psi(t) = \frac{\pi}{2} - \frac{\pi}{4}\sin(2\pi t)$$

This generates a **cycle-mean wing force** that is predominantly **perpendicular to the stroke plane**.

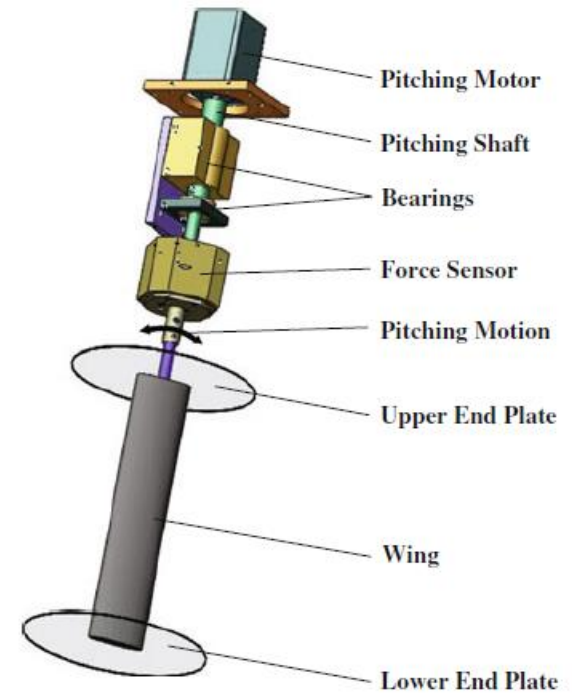


**Wing action in wing frame**

# 2D flapping-wing test rig and load cell

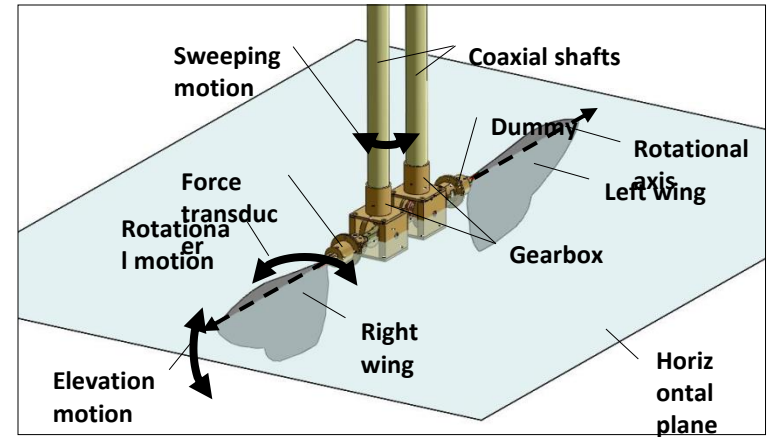
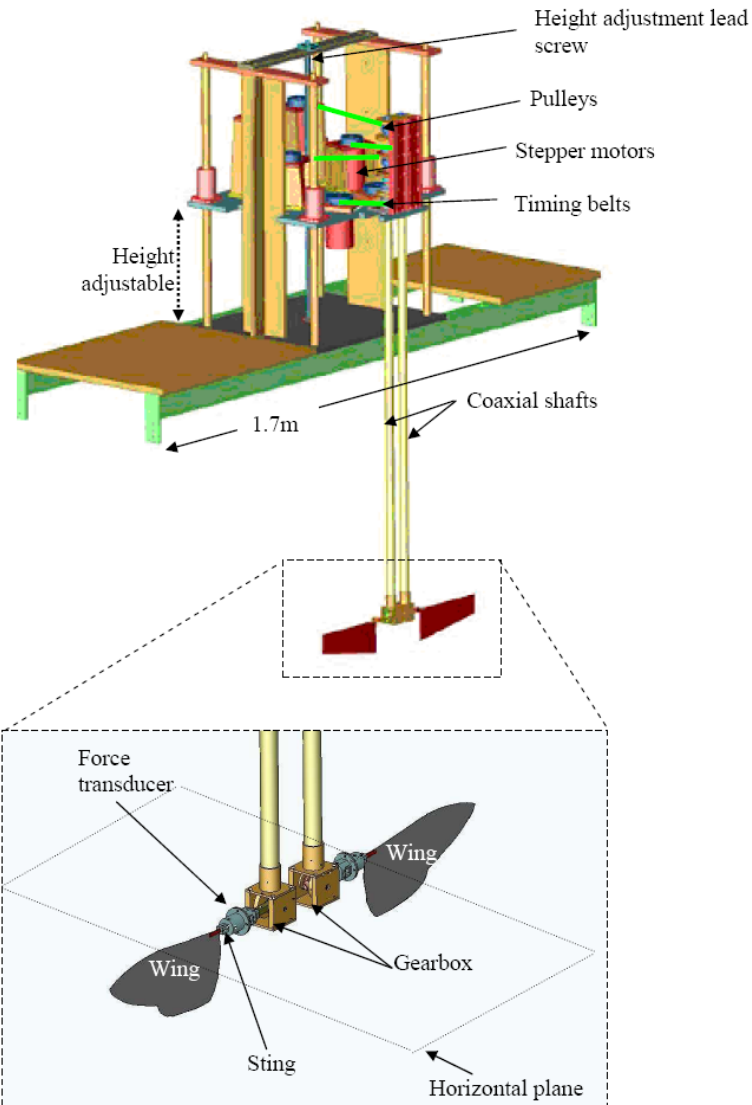


Actuation mechanism and DPIV setup

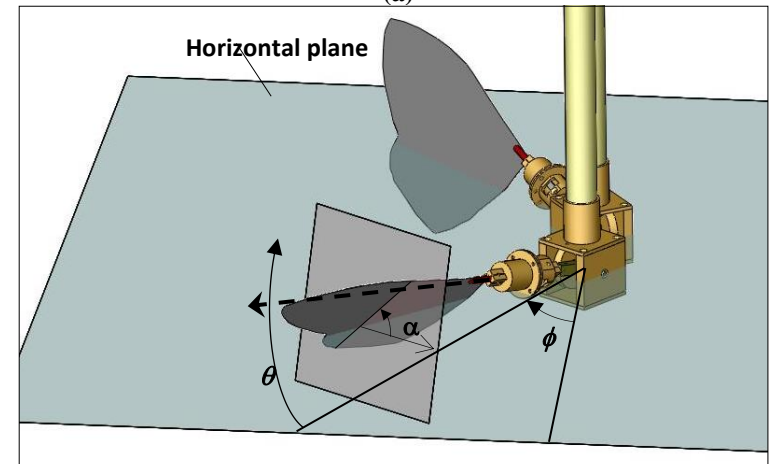


2D Wing pitching sub-assembly and force sensor

# 3D Flapping-wing test facility



(a)

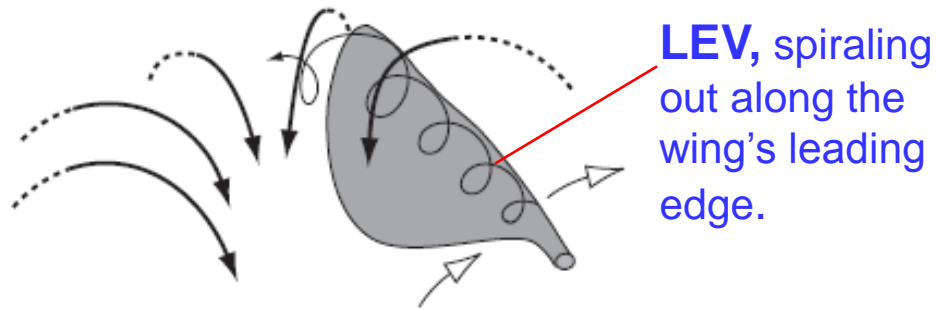


(b)

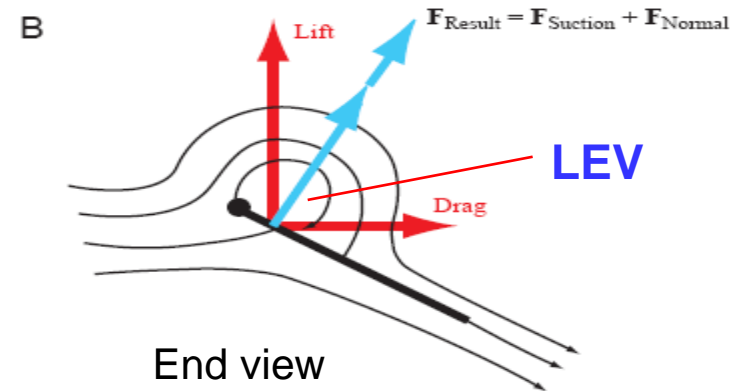
Fig. 2 Definition of coordinate system for the 3 axis of motion. (a) shows the definition of the flapping motions, and (b) shows the definition of angle of attack  $\alpha$ , elevation angle  $\theta$  and positional angle  $\phi$ .

## Leading-edge vortex (LEV)

At large angle of attack typical of flapping wings, flow separation may occur at the leading edge and wing tip regions of the wings resulting in the formation of a strong **leading-edge vortex (LEV)** above the wing.



From Sane S.P. (2003) *J. Exp. Biol.* **206**, 4191-4208.

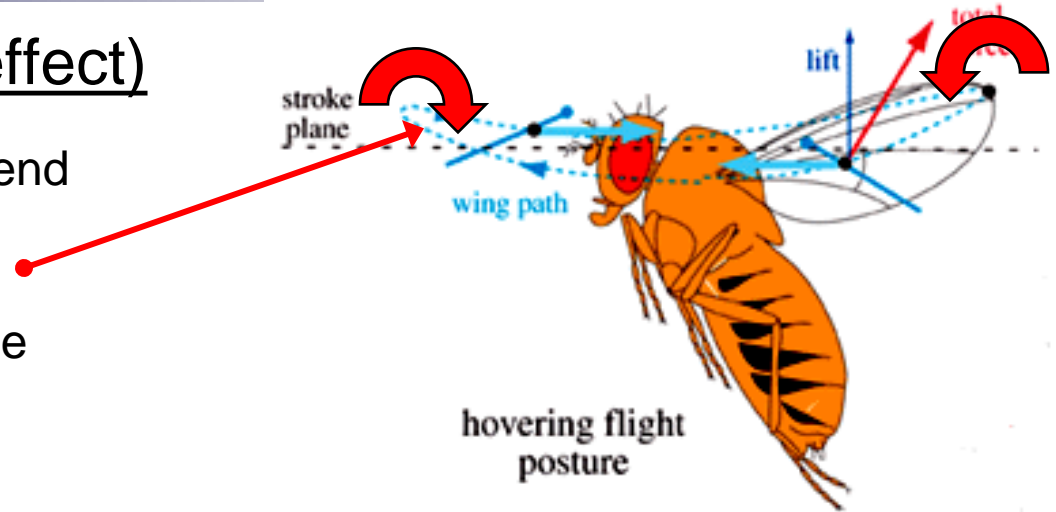


Strong vortical flow in the LEV leads to reduced pressure in the LEV over the wings; thus producing extra lift effect due to suction effect.



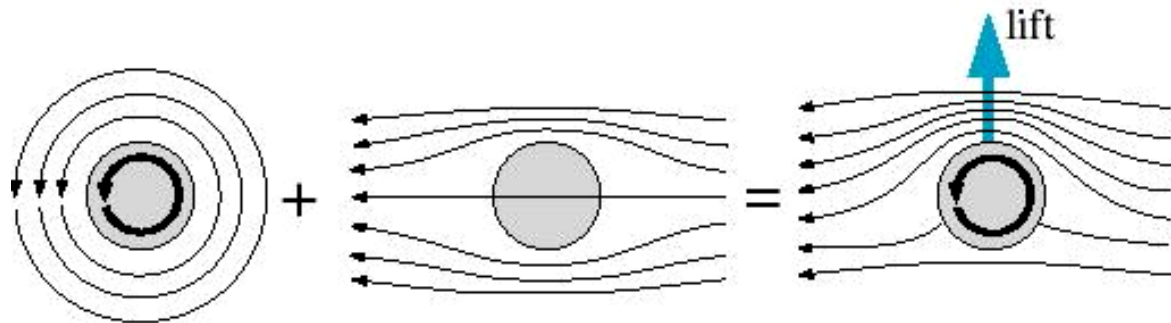
# Rotational Lift: (Magnus effect)

Rapid rotation of the wings at the end of a wing stroke can produce substantial rotational flow – this combines with the translation of the wing to produce extra lift.



(From Dickinson, Berkeley)

## rotation lift

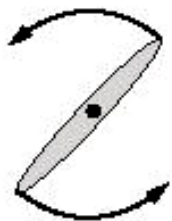


Lift generated by cylinder due to rotation cum translation to the right

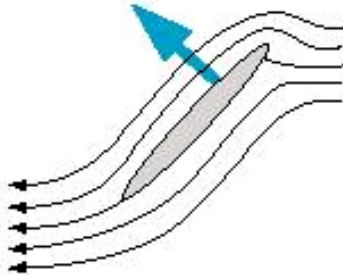
rotation

translation

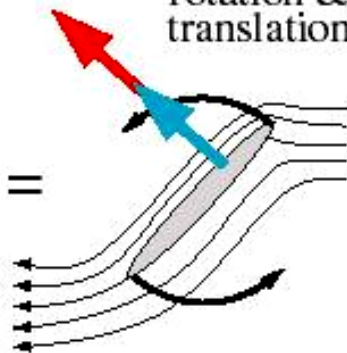
rotation & translation



+



=



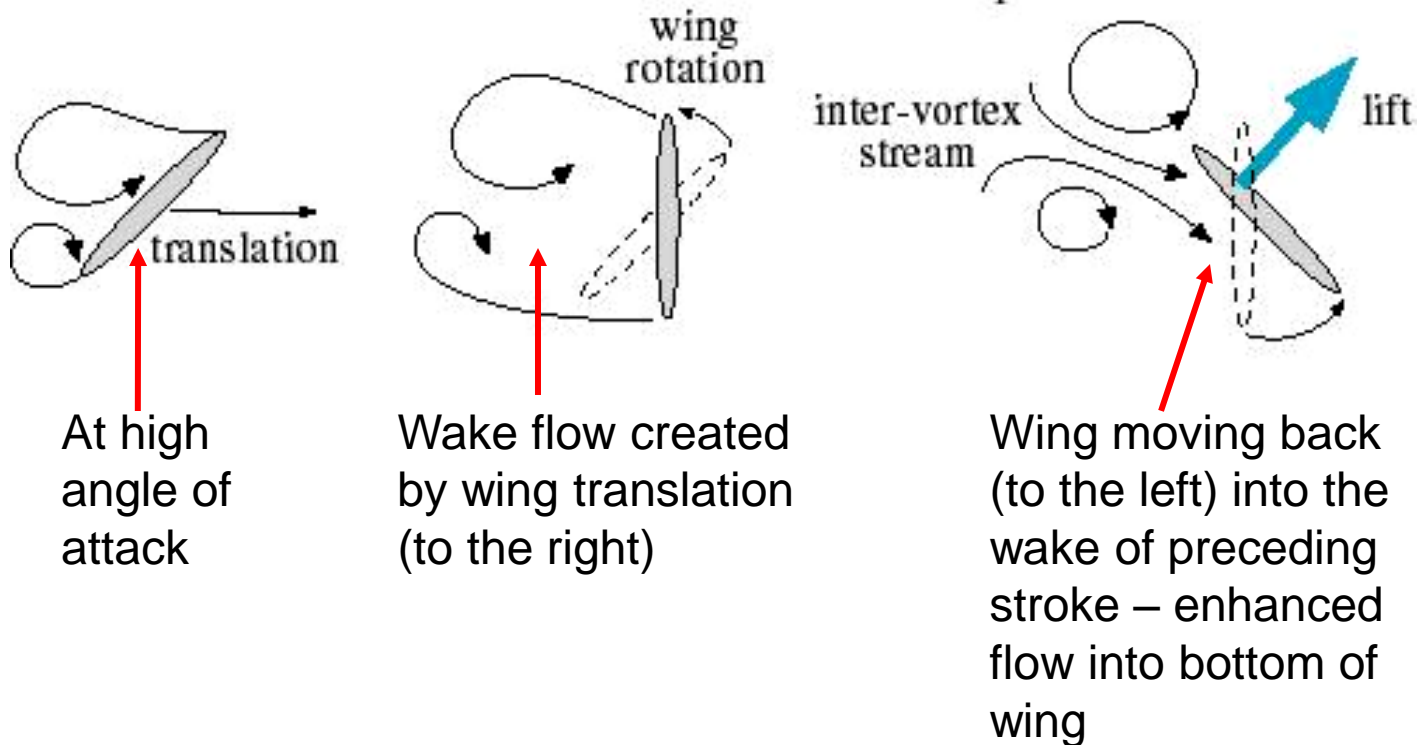
Additional lift produced by wing rotation cum translation to the right

# Wake Capture

This involves subsequent action of the wings utilizing flow (wake) produced by a precedent action of the wing to enhance lift. For example:

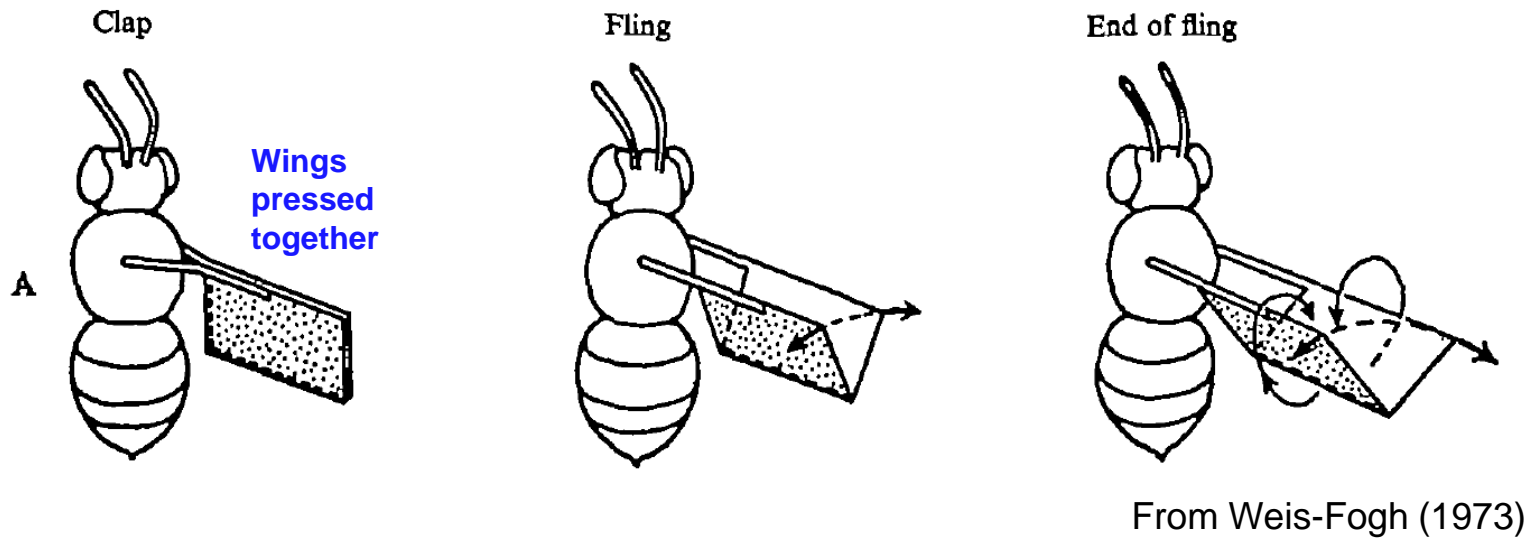
## *Wake Capture*

(From Dickinson)



## Clap and Fling mechanism

This mechanism was first identified by Weis-Fogh (1973) in very small insects, such as the *Encarsia Formosa* (a small wasp with wingspan of 1 mm), to generate high lift ( $C_L \approx 2-3.5$ ) at low  $Re \approx 10-20$ .



This involves the wings being clapped together and then fling apart with the trailing edges of the wing in close contact.